

Sterically Crowded *peri*-Substituted Naphthalene Phosphines and their P^V Derivatives

Fergus R. Knight, Amy L. Fuller, Michael Bühl, Alexandra M. Z. Slawin, and J. Derek Woollins*^[a]

Abstract: Three sterically crowded *peri*-substituted naphthalene phosphines, Nap[PPh₂][ER] (Nap = naphthalene-1,8-diyl; ER = SEt, SPh, SePh) **1–3**, which contain phosphorus and chalcogen functional groups at the *peri* positions have been prepared. Each phosphine reacts to form a complete series of P^V chalcogenides Nap[P(E')-(Ph₂)(ER)] (E' = O, S, Se). The novel compounds were fully characterised by using X-ray crystallography and multinuclear NMR spectroscopy, IR spectroscopy and MS. X-ray data for **1**, **2**, **nO**, **nS**, **nSe** (*n* = 1–3) are compared. Eleven molecular structures have been

analysed by naphthalene ring torsions, *peri*-atom displacement, splay angle magnitude, X⋯E interactions, aromatic ring orientations and quasi-linear arrangements. An increase in the congestion of the *peri* region following the introduction of heavy chalcogen atoms is accompanied by a general increase in naphthalene distortion. P⋯E distances increase for molecules that contain

Keywords: chalcogens • density functional calculations • intramolecular interactions • oxidation • *peri*-substitution • X-ray diffraction

bulkier atoms at the *peri* positions and also when larger chalcogen atoms are bound to phosphorus. The chalcogenides adopt similar conformations that contain a quasi-linear E⋯P–C fragment, except for **3O**, which displays a twist-axial-twist conformation resulting in the formation of a linear O⋯Se–C alignment. Ab initio MO calculations performed on **2O**, **3O**, **3S** and **3Se** reveal Wiberg bond index values of 0.02 to 0.04, which indicates only minor non-bonded interactions; however, calculations on radical cations of **3O**, **3S** and **3Se** reveal increased values (0.14–0.19).

Introduction

peri-Substituted naphthalenes incorporating large heteroatoms confined in close proximity with separations shorter than the sum of the van der Waals (vdW) radii have received great attention.^[1] Un-substituted (“ideal”) naphthalene is known to be rigidly planar with unequal bond lengths and bond angles.^[2] The *peri*-carbon atoms are separated by a distance of 2.44 Å,^[2] which is sufficient to accommodate two hydrogen atoms, but it is reasonable to expect that there will be considerable steric hindrance with larger sub-

stituents occupying the *peri* positions.^[3] Repulsive steric effects caused by the crowding of substituents can be overcome by attractive weak or strong intramolecular interactions, or by the deformation of the naphthalene skeleton away from ideal.^[3,4] This gives rise to structurally distorted compounds with unusual bonding and geometry.^[3]

X-ray structural data has played a crucial role when analysing the extent of steric strain and the amount of distortion occurring in non-ideal naphthalenes and has helped to elucidate attractive effects between *peri* atoms and verify the existence of weak intra- and intermolecular interactions.^[4] To quantify the extent of naphthalene distortion taking place in a given molecule, the naphthalene geometry is compared with that of ideal or un-substituted naphthalene.^[2,5,6]

Steric strain operating between crowded *peri* atoms can also be relieved by coordination of the bidentate ligand to a bridging metal centre, forming a stable ring complex (chelate).^[7] Phosphines, being neutral two-electron donors, are one of the most versatile ligands that can bind to late-transition metals.^[8] The complexes they form are important in organic synthesis and have been shown to act as active homog-

[a] F. R. Knight, Dr. A. L. Fuller, Dr. M. Bühl, Prof. A. M. Z. Slawin, Prof. J. D. Woollins
School of Chemistry
University of St Andrews
St Andrews, Fife
KY16 9ST (UK)
Fax: (+44) 1334-463384
E-mail: jdww3@st-and.ac.uk

Supporting information for this article is available on the WWW under <http://dx.doi.org/10.1002/chem.201000454>, and contains X-ray crystallographic data for compounds **1**, **2**, **nO**, **nS** and **nSe** (*n* = 1–3).

eneous catalysts in reactions of industrial importance.^[9] The development of a novel class of 1,8-bisphosphine bidentate ligand that uses the rigid C_3 naphthalene backbone and positions phosphino groups *peri*-substituted on the ring has received great attention over the last 30 years.^[1c,10]

Extensive work has also been carried out on mixed donor phosphorus–nitrogen compounds.^[11] A leading topic of current research and one which has seen much controversy, concerns the possible occurrence of intramolecular dative bond formation leading to hypercoordination.^[11,12] Most of the pertinent work in this field has been performed by using 8-dimethylaminonaphth-1-yl (DAN) compounds in which the nitrogen atom can donate a pair of electrons in the formation of a coordination bond with acceptor heteroatoms, such as Si or P.^[13] Upon bond formation, the acceptor species finds itself with a greater than normal co-ordination number and is termed “hypercoordinate”.^[13]

Unlike bis-phosphines and DAN–phosphorus compounds, phosphorus–oxygen, phosphorus–sulfur and phosphorus–selenium *peri*-substituted naphthalenes have received limited attention in the literature. These exciting new phosphorus ligands provide good models with which to study naphthalene distortion, intramolecular interactions (including possible dative bonding and hypercoordination) and metal complexation. The difference in the electronic properties between the donor atoms of the new (P,O), (P,S) and (P,Se) systems means these compounds could also be of value as hemi-labile ligands.^[14]

During our early studies of sterically crowded 1,8-disubstituted naphthalenes we investigated dichalcogenide ligands^[15] and unusual phosphorus compounds.^[7,16] More recently we reported the synthesis and structural study of mixed halogen–chalcogen^[5] and chalcogen–chalcogen^[6] systems and the preparation of a novel mixed-donor phosphorus–oxygen ligand.^[17] A preliminary study of the coordination chemistry of novel phosphorus–sulfur ligand **2** has also been presented.^[18]

Herein we report the synthesis and a comprehensive structural study of (8-phenylsulfanyl)naphth-1-yl)diphenylphosphine **2**,^[18] along with two analogous mixed phosphorus–chalcogen *peri*-substituted systems, (8-ethylsulfanyl)naphth-1-yl)diphenylphosphine **1** and (8-phenylselanyl)naphth-1-yl)diphenylphosphine **3**.^[19] Compounds **1–3** react to form complete series of mono-oxidised oxygen, sulfur and selenium derivatives, and the synthesis and molecular study of these nine compounds is also presented (Figure 1).

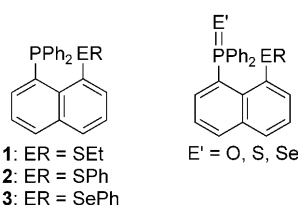


Figure 1. Sterically crowded *peri*-substituted naphthalene phosphines **1–3** and their phosphorus(V) oxygen, sulfur and selenium derivatives **nO**, **nS**, **nSe** ($n=1–3$).

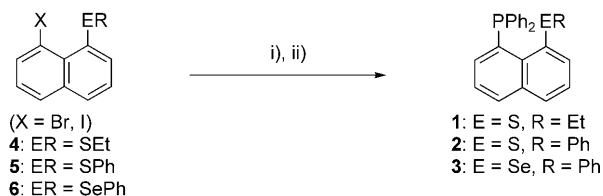
Results and Discussion

Compounds **1–3** and their chalcogeno derivatives were synthesised and crystal structures were determined for **1**, **2**, **nO**, **nS** and **nSe** ($n=1–3$). All derivatives were spectrally characterised by multinuclear NMR and IR spectroscopy and mass spectrometry and the homogeneity of the new compounds was, where possible, confirmed by microanalysis. ³¹P and ⁷⁷Se NMR spectroscopy data for all compounds is displayed in Table 1.

Table 1. ³¹P and ⁷⁷Se NMR spectroscopic data (δ [ppm], J [Hz]) for phosphines **1–3** and related chalcogeno derivatives.

	1	1O	1S	1Se
δ_P	–5	36	52	42
δ_{Se}	n/a	n/a	n/a	–172
	2	2O	2S	2Se
δ_P	–5	37	53	42
δ_{Se}	n/a	n/a	n/a	–341
$^1J(P,Se)$	n/a	n/a	n/a	722
	3	3O	3S	3Se
δ_P	–13	38	51	41
δ_{Se}	n/a	n/a	n/a	–163
δ_{Se}	440	450	449	451
$^4J(P,Se)$	391	n/a	19	24
$^1J(P,Se)$	n/a	n/a	n/a	715

We recently reported the synthesis of a series of 1-halo-8-(alkylchalcogeno)naphthalene derivatives (**4–5**) prepared from the stepwise halogen–lithium exchange reactions of analogous 1,8-dibromonaphthalene and 1,8-diiodonaphthalene.^[5] These compounds are ideal intermediates in the preparation of phosphorus–chalcogen *peri*-substituted systems **1–3**. For the synthesis, the respective halogen–chalcogen compound was treated with a single equivalent of *n*-butyllithium in diethyl ether to afford the respective 1-lithio-8-(phenylchalcogeno)naphthalene precursor. Treatment with a single equivalent of chlorodiphenylphosphine under standard reactions conditions^[20] afforded the respective *peri*-substituted naphthalene phosphines **1–3** (yields based on the bromo and iodo starting material, respectively: **1** 11 and 51%; **2** 64 and 74%, **3** 40 and 60%; Scheme 1).

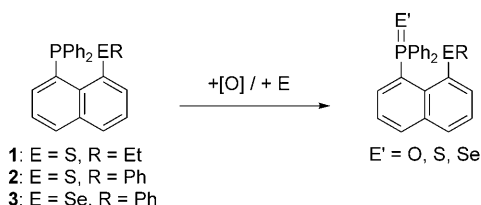


Scheme 1. The preparation of (8-alkylchalcogenonaphth-1-yl)diphenylphosphines **1–3**. Conditions: i) *n*BuLi (1 equiv), Et₂O, –78 °C, 1 h; ii) CIPPh₂ (1 equiv), Et₂O, –78 °C, 1 h.

Compounds **1–3** were characterised by elemental analysis, IR spectroscopy, ¹H, ¹³C and ³¹P NMR spectroscopy and mass spectrometry. Compound **3** was analysed by using

^{77}Se NMR spectroscopy. Similar chemical shifts were observed in the ^{31}P NMR spectra of sulfur compounds **1** ($\delta_{\text{P}} = -5.24$ ppm) and **2** ($\delta_{\text{P}} = -5.30$ ppm). The ^{31}P and ^{77}Se NMR spectra for **3** ($\delta_{\text{P}} = -12.94$ ppm; $\delta_{\text{Se}} = 439.6$ ppm; $^4J(\text{P,Se}) = 391.0$ Hz) are in accord with literature values ($\delta_{\text{P}} = -12.51$ ppm; $\delta_{\text{Se}} = 446.2$ ppm; $^4J(\text{P,Se}) = 380.9$ Hz;^[19] see Table 1).

Phosphines **1–3** react to form a series of three phosphorus(V) chalcogenide derivatives. In each case, under atmospheric conditions, the three-coordinate phosphorus atom is readily oxidised to four-coordinate phosphine oxides **1O**, **2O** and **3O** (Scheme 2). Similarly, the treatment of **1–3** with



Scheme 2. The preparation of the phosphorus(V) chalcogenide derivatives of **1–3**. Conditions: Toluene, 80 °C.

stoichiometric amounts of sulfur and selenium powder under reflux selectively affords novel sulfides **1S**, **2S**, **3S** and selenides **1Se**, **2Se**, **3Se**, respectively. Conversion of **1–3** to the respective P^{V} chalcogenide derivative was achieved in 100% yield in each case, as observed by ^1H and ^{31}P NMR spectroscopy.

The P^{V} chalcogenides were characterised by elemental analysis, IR spectroscopy, ^1H , ^{13}C and ^{31}P NMR spectroscopy and mass spectrometry. Compounds **1Se**, **2Se**, **3O**, **3S** and **3Se** were analysed by using ^{77}Se NMR spectroscopy. Characterisation data for **3O** ($\delta_{\text{P}} = 37.99$ ppm; $\delta_{\text{Se}} = 450.4$ ppm) were found to be in accord with the literature values (lit.: $\delta_{\text{P}} = 37.47$ ppm; $\delta_{\text{Se}} = 457.9$ ppm).^[19]

A downfield shift was observed in the $^{31}\text{P}\{^1\text{H}\}$ NMR spectra of the four-coordinate phosphorus compounds compared to the chemical shifts of the three-coordinate phosphines **1–3**. $^{31}\text{P}\{^1\text{H}\}$ NMR spectra showed single peaks at comparable shifts for the oxides ($\delta_{\text{P}} = 36.34$ (**1O**), 37.01 (**2O**), 37.99 ppm (**3O**)), sulfides ($\delta_{\text{P}} = 51.84$ (**1S**), 52.52 (**2S**), 51.01 ppm (**3Se**)) and selenides ($\delta_{\text{P}} = 41.92$ (**1Se**), 42.46 (**2Se**), 40.50 ppm (**3Se**)). Expected 1J and 4J values for phosphorus–selenium coupling were observed in the spectra of **3Se** ($^1J(\text{P,Se}) = 715.3$ Hz, $^4J(\text{P,Se}) = 23.9$ Hz), though $^1J(\text{P,Se})$ coupling was not observed in the spectra of **1Se** or **2Se** and $^4J(\text{P,Se})$ coupling was not observed in the spectra of **3O** and **3S** (Table 1).

Single peaks in the ^{77}Se NMR spectra of **1Se**, **2Se** and **3O** displayed no $J(\text{Se,P})$ coupling. The ^{77}Se NMR spectrum for **3S** displayed a doublet at $\delta = 448.5$ ppm with a small $^4J(\text{Se,P})$ coupling value of 19.1 Hz. Two sharp doublets were observed in the ^{77}Se NMR spectrum of **3Se** ($\delta = 451.4$ and -162.8 ppm), with 1J and 4J values for selenium–phosphorus coupling of 715 and 24 Hz, respectively (Table 1).

X-ray investigations: Compound **3** is an oil at room temperature, but suitable single crystals were obtained for all other derivatives by diffusion of pentane into saturated solutions of the individual compound in dichloromethane. The molecular structures were analysed, although **2**^[18] and **3O**^[19] have been previously reported. Compound **1** crystallises with two nearly identical molecules in the asymmetric unit, all other compounds contain one molecule in the asymmetric unit. Selected interatomic distances, angles and torsion angles are listed in Tables 2 and 3. Further crystallographic information can be found in Tables 7, 8 and 9 and the Supporting Information.

The molecular structures of **1** and **2** are shown in Figures 2 and 3, respectively. Overall, the degree of steric strain operating between the *peri* atoms in S(ethyl) derivative **1** is

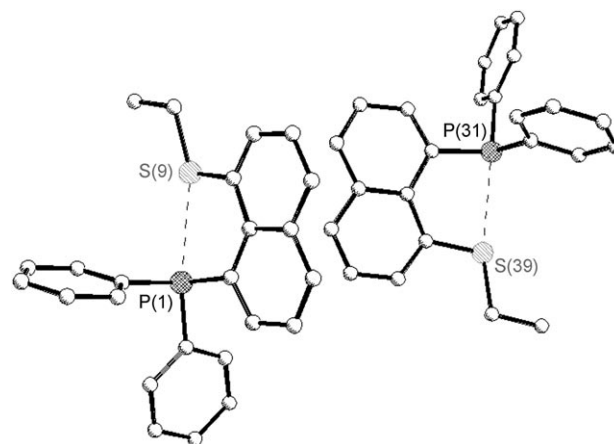


Figure 2. The crystal structure of (8-ethylsulfanylnaphth-1-yl)diphenylphosphine **1** showing two independent molecules in the asymmetric unit.

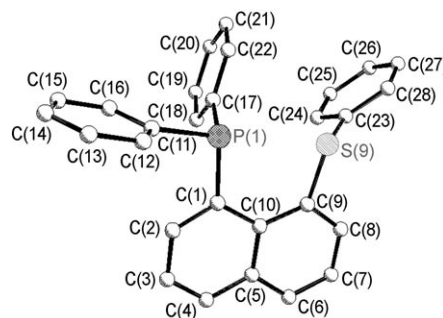


Figure 3. The crystal structure of (8-phenylsulfanylnaphth-1-yl)diphenylphosphine **2**.^[18]

notably reduced compared to the S(phenyl) analogue **2**. The displacement of the *peri* atoms to opposite sides of the mean naphthalene plane occurs to a slightly unequal degree in the two independent plane molecules of **1** (-0.11 (0.05), 0.16 Å (-0.03 Å)). In compound **2** (0.007, 0.13 Å),^[18] the phosphorus atom lies virtually on the naphthyl plane. Positive splay angles are observed for both compounds **1** (11.7 (11.4°)) and **2** (14.1 , 18°), but there is a notable increase in the splay of

Table 2. Selected interatomic distances [\AA] and angles [$^\circ$] for **1**, **10**, **1S** and **1Se**.^[a]

	1	10	1S	1Se
<i>peri</i> -Region distances and sub-vdW contacts in the <i>peri</i> region				
P(1)⋯S(1)	2.9737(14) (2.9469(15))	3.1349(13)	3.2083(14)	3.2283(19)
$\Sigma r_{\text{vdW}}-\text{P}\cdots\text{S}^{[\text{b}]}$	0.6263 (0.6531)	0.4651	0.3917	0.3717
$\Sigma r_{\text{vdW}}^{[\text{b}]} [\%]$	83 (82)	87	89	90
P(1)–C(1)	1.838(4) (1.848(3))	1.832(3)	1.837(3)	1.843(5)
S(1)–C(9)	1.779(4) (1.776(4))	1.772(3)	1.783(4)	1.771(6)
P(1)=E(2)	–	1.487(2)	1.9550(14)	2.1103(17)
S(1)⋯E(2)	–	3.033(2)	3.2951(15)	3.43(1)
$\Sigma r_{\text{vdW}}-\text{S}\cdots\text{E}^{[\text{b}]}$	–	0.287	0.305	0.270
$\Sigma r_{\text{vdW}}^{[\text{b}]} [\%]$	–	91	92	93
Naphthalene bond lengths				
C(1)–C(2)	1.383(4) (1.373(5))	1.382(5)	1.384(5)	1.364(6)
C(2)–C(3)	1.406(5) (1.416(5))	1.387(5)	1.411(5)	1.408(8)
C(3)–C(4)	1.367(5) (1.355(5))	1.369(5)	1.360(5)	1.358(7)
C(4)–C(5)	1.413(5) (1.413(5))	1.418(5)	1.412(5)	1.417(6)
C(5)–C(10)	1.445(5) (1.438(5))	1.426(5)	1.430(5)	1.434(7)
C(5)–C(6)	1.424(5) (1.416(6))	1.411(5)	1.420(5)	1.401(7)
C(6)–C(7)	1.356(5) (1.338(6))	1.368(5)	1.365(6)	1.373(7)
C(7)–C(8)	1.400(5) (1.410(6))	1.386(6)	1.408(6)	1.397(8)
C(8)–C(9)	1.367(5) (1.379(5))	1.379(5)	1.377(5)	1.378(7)
C(9)–C(10)	1.461(5) (1.438(5))	1.439(5)	1.443(5)	1.443(6)
C(10)–C(1)	1.442(5) (1.466(5))	1.444(4)	1.438(5)	1.456(6)
<i>peri</i> -Region bond angles				
P(1)–C(1)–C(10)	123.6(3) (122.4(3))	123.9(2)	124.5(2)	124.2(3)
C(1)–C(10)–C(9)	126.9(3) (126.0(3))	126.5(3)	126.0(3)	127.2(4)
S(1)–C(9)–C(10)	121.2(3) (123.0(3))	122.7(2)	121.4(2)	122.4(4)
Σ of bay angles	371.7 (371.4)	373.1	371.9	373.8
Splay angle ^[c]	11.7 (11.4)	13.1	11.9	13.8
C(4)–C(5)–C(6)	118.1(4) (118.9(4))	118.2(3)	119.4(3)	118.7(5)
S(1)⋯P(1)–C(11)	163.3(1) (160.6(1))	174.3(1)	175.4(1)	170.9(1)
Out-of-plane displacement				
P(1)	–0.11(1) (0.05(1))	–0.566(4)	–0.620(4)	–0.599(7)
S(1)	0.16(1) (–0.03(1))	0.404(4)	0.744(4)	0.527(6)
E(2)	–	–1.720(5)	–2.019(5)	–2.302(7)
Central naphthalene ring torsion angles				
C(6)–C(5)–C(10)–C(1)	–177.1(3) (179.8(4))	175.4(3)	–168.4(3)	–173.7(6)
C(4)–C(5)–C(10)–C(9)	–176.5(3) (–177.2(4))	175.0(3)	–171.0(3)	–175.3(6)

[a] Values in parentheses are for independent molecules. [b] vdW radii used for calculations: $r_{\text{vdW}}(\text{P})$ 1.80 \AA , $r_{\text{vdW}}(\text{O})$ 1.52 \AA , $r_{\text{vdW}}(\text{S})$ 1.80 \AA , $r_{\text{vdW}}(\text{Se})$ 1.90. ^[21] [c] Splay angle: Σ of the three bay region angles –360.

the P–C and S–C bonds in the S(phenyl) derivative to alleviate the greater “*peri*-space crowding”.^[22]

The resulting geometry repels the P and S atoms to a greater non-bonded interatomic distance of 3.0330(7) \AA in **2**^[18] as compared with the S(ethyl) derivative **1** (2.9737(14) \AA (2.9469(15) \AA)). The *peri* gap in both cases is still 16 to 18% shorter than the sum of their collective vdW radii. The naphthalene units for both derivatives show only minor deviations from planarity with maximum C–C–C central naphthalene ring torsion angles of around 0 to 4°. Repulsive forces acting between the P and S atoms are accompanied by C–C bond and C–C–C angle stretching in the naphthalene scaffold. Bond lengths around C(10), closer to the repulsive forces, are on average longer than those around C(5) (average 1.45 and 1.42 \AA , respectively) and C(1)–C(10)–C(9) bond angles splay to a mean 127°, wider than the ideal geometry observed for C(4)–C(5)–C(6) (average 119°).^[2] S–C (1.78–1.82 \AA) and P–C (1.83–1.86 \AA) bond lengths are within the usual ranges ((1.77 ± 0.05), (1.84 ± 0.05) \AA , respectively)^[23] in both cases.

The geometrical structures of compounds **1** and **2** can be described by the conformation and arrangement of the naphthyl ring and ethyl/phenyl groups relative to the two C(ar)–P(1)–C(ar) planes and the C(ar)–S(1)–C(R) plane. This can be categorised from torsion angles θ and γ , respectively (see Table 4). When θ and γ approach 90° the orientation is denoted axial and when the angles indicate a quasi-planar arrangement (close to 180°), they are termed equatorial.^[24] When angle θ is axial, the respective P–C_{Ph}/S–C_R bond lies perpendicular to the naphthyl plane whereas an equatorial conformation aligns the bond on or close to the plane. Based on the classification system presented by Nakanishi et al.,^[25] axial conformations of angle θ correspond to a type -A structure and equatorial to type B. The twist conformation is thus type C.^[24, 25] From the nomenclature reported by Nakanishi et al.,^[25] compounds **1** and **2** can thus be described as type BA-B and BA-C-c, respectively (c denotes a *cis* orientation of phenyl groups with respect to the naphthyl plane; see Figure 4).^[25] One quasi-linear

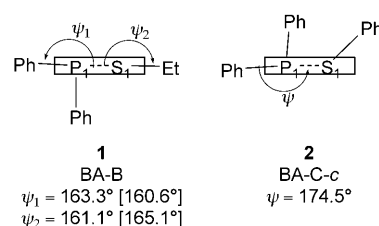


Figure 4. The orientation of the phenyl and ethyl groups, the structure type and the quasi-linear arrangements of **1** and **2**.^[25]

arrangement (S(1)⋯P(1)–C(11)) with an angle of 174.5° is observed in **2**, whereas two linear arrangements (S(1)⋯P(1)–C(11) and P(1)⋯S(1)–C(23)) with angles of 163.3 (160.6) and 161.1° (165.1°), respectively, are observed in **1**.

The BA-C-c conformation in **2** places one of the P(phenyl) groups and the (S)phenyl group on the same side

Table 3. Selected interatomic distances [Å] and angles [°] for **2**, **2O**, **2S**, **2Se**, **3O**, **3S** and **3Se**.

	2	2O	2S	2Se	3O	3S	3Se
<i>peri</i> -Region distances and sub-vdW contacts in <i>peri</i> region							
P(1)⋯E(1)	3.0330(7)	3.1489(9)	3.191(1)	3.190(1)	3.215(2)	3.2803(8)	3.278(2)
$\Sigma r_{\text{vdW}}-\text{P}\cdots\text{E}^{[\text{a}]}$	0.567	0.4511	0.409	0.410	0.485	0.4197	0.422
$\Sigma r_{\text{vdW}}^{[\text{a}]}$ [%]	84	87	89	89	89	89	89
P(1)–C(1)	1.8548(19)	1.835(3)	1.837(3)	1.836(4)	1.826(5)	1.837(3)	1.825(6)
E(1)–C(9)	1.785(2)	1.777(3)	1.779(3)	1.782(4)	1.937(4)	1.916(3)	1.917(6)
P(1)=E(2)	–	1.492(2)	1.9585(12)	2.1181(11)	1.476(4)	1.9567(10)	2.1165(16)
E(1)⋯E(2)	–	2.9612(17)	3.3142(11)	3.3974(10)	2.770(3)	3.3490(7)	3.4217(8)
$\Sigma r_{\text{vdW}}-\text{E}\cdots\text{E}$	–	0.3588	0.2858	0.3026	0.65	0.351	0.3783
$\Sigma r_{\text{vdW}}^{[\text{a}]}$ [%]	–	89	92	92	81	91	90
Naphthalene bond lengths							
C(1)–C(2)	1.376(3)	1.380(5)	1.376(5)	1.385(5)	1.358(7)	1.385(4)	1.387(8)
C(2)–C(3)	1.404(3)	1.400(5)	1.414(5)	1.400(6)	1.423(7)	1.397(4)	1.417(9)
C(3)–C(4)	1.353(3)	1.365(5)	1.352(4)	1.363(6)	1.344(8)	1.354(4)	1.341(9)
C(4)–C(5)	1.415(3)	1.419(5)	1.422(5)	1.422(6)	1.410(8)	1.413(4)	1.416(9)
C(5)–C(10)	1.442(3)	1.430(5)	1.435(4)	1.431(6)	1.439(7)	1.429(4)	1.441(9)
C(5)–C(6)	1.420(3)	1.420(4)	1.419(4)	1.411(5)	1.425(8)	1.418(4)	1.419(8)
C(6)–C(7)	1.358(3)	1.355(5)	1.345(5)	1.356(7)	1.368(8)	1.347(4)	1.359(10)
C(7)–C(8)	1.399(3)	1.408(5)	1.401(5)	1.390(6)	1.398(7)	1.402(4)	1.387(10)
C(8)–C(9)	1.377(3)	1.376(4)	1.372(4)	1.372(5)	1.384(7)	1.389(4)	1.396(8)
C(9)–C(10)	1.437(3)	1.432(4)	1.433(4)	1.431(5)	1.409(6)	1.433(4)	1.437(9)
C(10)–C(1)	1.448(3)	1.443(4)	1.452(4)	1.454(5)	1.455(7)	1.450(3)	1.437(8)
<i>peri</i> -Region bond angles							
P(1)–C(1)–C(10)	124.07(13)	124.6(2)	124.2(2)	125.0(3)	123.6(3)	125.4(2)	126.5(4)
C(1)–C(10)–C(9)	126.90(17)	126.2(3)	127.3(3)	126.6(3)	126.8(4)	126.7(2)	126.3(5)
E(1)–C(9)–C(10)	123.11(13)	121.6(2)	122.2(2)	122.5(3)	125.1(3)	124.7(2)	124.5(4)
Σ of bay angles	374.1	372.4	373.7	374.1	375.5	376.8	377.3
Splay angle ^[b]	14.1	12.4	13.7	14.1	15.5	16.8	17.3
C(4)–C(5)–C(6)	118.60(18)	119.6(3)	118.9(3)	119.0(4)	119.8(4)	118.6(2)	118.9(6)
E(1)⋯P(1)–C(11)	174.5(1)	177.6(1)	174.0(1)	173.8(1)	167.9(1)	173.5(1)	172.9(1)
E(2)⋯E(1)–C(23)	–	145.4(1)	145.8(1)	149.1(1)	178.1(1)	145.0(1)	148.4(1)
Out-of-plane displacement							
P(1)	0.007(1)	0.6312(37)	0.633(4)	0.621(47)	–0.578(6)	0.601(3)	0.578(7)
E(1)	0.127(1)	–0.582(4)	–0.451(4)	–0.433(5)	0.450(6)	–0.420(3)	–0.397(7)
E(2)	–	1.6231(46)	2.1977(43)	2.3457(51)	–1.458(8)	2.179(4)	2.314(8)
Central naphthalene ring torsion angles							
C(6)–C(5)–C(10)–C(1)	178.49(16)	171.7(2)	173.7(2)	175.4(3)	174.4(5)	174.9(2)	175.7(5)
C(4)–C(5)–C(10)–C(9)	–179.5(2)	170.3(2)	173.4(2)	173.1(3)	170.5(5)	173.6(2)	175.1(5)

[a] vdW radii used for calculations: $r_{\text{vdW}}(\text{P})$ 1.80 Å, $r_{\text{vdW}}(\text{O})$ 1.52 Å, $r_{\text{vdW}}(\text{S})$ 1.80 Å, $r_{\text{vdW}}(\text{Se})$ 1.90.^[21] [b] Splay angle: Σ of the three bay region angles–360.

Table 4. Torsion angles [°] categorising the naphthalene and ethyl/phenyl ring conformations in **1** and **2**.^[a]

1		2	
Torsion angle	Conformation	Torsion angle	Conformation
Naphthalene ring conformations			
C(10)–C(1)–P(1)–C(11)	$\theta_1 = 167.8(1)$ (162.6(1))	Nap ₁ : equatorial	$\theta_2 = 177.0(1)$
C(10)–C(1)–P(1)–C(17)	$\theta_2 = -87.3(1)$ (–92.5(1))	Nap ₂ : axial	$\theta_2 = 78.6(1)$
C(10)–C(9)–S(1)–C(23)	$\theta_3 = 168.3(1)$ (169.5(1))	Nap ₃ : equatorial	$\theta_1 = -129.2(1)$
Ethyl/phenyl group conformations			
C(1)–P(1)–C(11)–C(12)	$\gamma_1 = 109.9(1)$ (96.1(1))	Ph ₁ : axial	$\gamma_1 = 92.6(11)$
C(1)–P(1)–C(17)–C(18)	$\gamma_2 = 158.1(1)$ (158.5(1))	Ph ₂ : equatorial	$\gamma_2 = 17.8(1)$
C(9)–S(1)–C(23)–C(24)	$\gamma_3 = -174.4(1)$ (–174.7(1))	Et ₁ : equatorial	$\gamma_3 = 48.0(1)$

[a] Values in parentheses are for independent molecules. Definitions: Nap₁: naphthalene ring P(1) relative to C₁–P₁–C₁₁; Nap₂: naphthalene ring P(1) relative to C₁–P₁–C₁₇; Nap₃: naphthalene ring S(1); Ph₁: P(1) phenyl ring 11–16; Ph₂: P(1) phenyl ring 17–22; Ph₃: S(1) phenyl ring; Et₁: S(1) ethyl group; axial: perpendicular to C(ar)–Z–C(R) plane; equatorial: coplanar with C(ar)–Z–C(R) plane; twist: intermediate between equatorial and axial.

of the naphthyl plane and in close proximity (Figure 4).^[25] The mixed axial-twist conformation of the two phenyl rings ($\gamma_1 = 92.6(11)^\circ$; $\gamma_3 = 48.0(1)^\circ$) results in no significant overlap and with a centroid–centroid distance of 4.32 Å, which is

much higher than for known π – π stacking (3.3–3.8 Å),^[26] no π – π interactions are observed.

All non-hydrogen atoms are larger in size than a lone pair of electrons, thus it is perhaps not surprising that an increase in steric strain is observed in chalcogenide derivatives **nO**, **nS** and **nSe** ($n = 1–3$) in which O, S and Se atoms crowd the *peri* space instead of the lone-pair in phosphanyl compounds **1–3**. The heavy chalcogen atoms are accommodated by a greater de-

formation of the naphthalene geometry through an increase in-plane and out-of-plane distortions and a significant twisting of the naphthalene skeleton.

The degree of distortion is generally related to the size of the atoms residing in the *peri* region. This is best observed by comparing the magnitude of the *peri*-distance parameter (Tables 2 and 3, Figure 5). In each set of chalcogenide derivatives there is a marked lengthening of the *peri* gap as larger atoms bind to phosphorus. The separation of the *peri* atoms in selenium compounds **3O**, **3S** and **3Se** is also notably larger compared with the derivatives of sulfur compounds **1** and **2** (Figure 5). P...E distances (3.12–3.28 Å) are less than the respective sum of vdW radii for the two *peri* atoms (3.60–3.70 Å);^[21] in all cases this is between 87 and 90% of the vdW sum. For derivatives of **1** and **2**, this is an

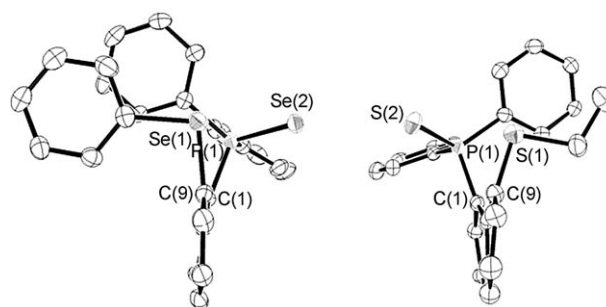


Figure 6. The least and most distorted naphthalene units for P^V chalcogenides **3Se** and **1S**, respectively.

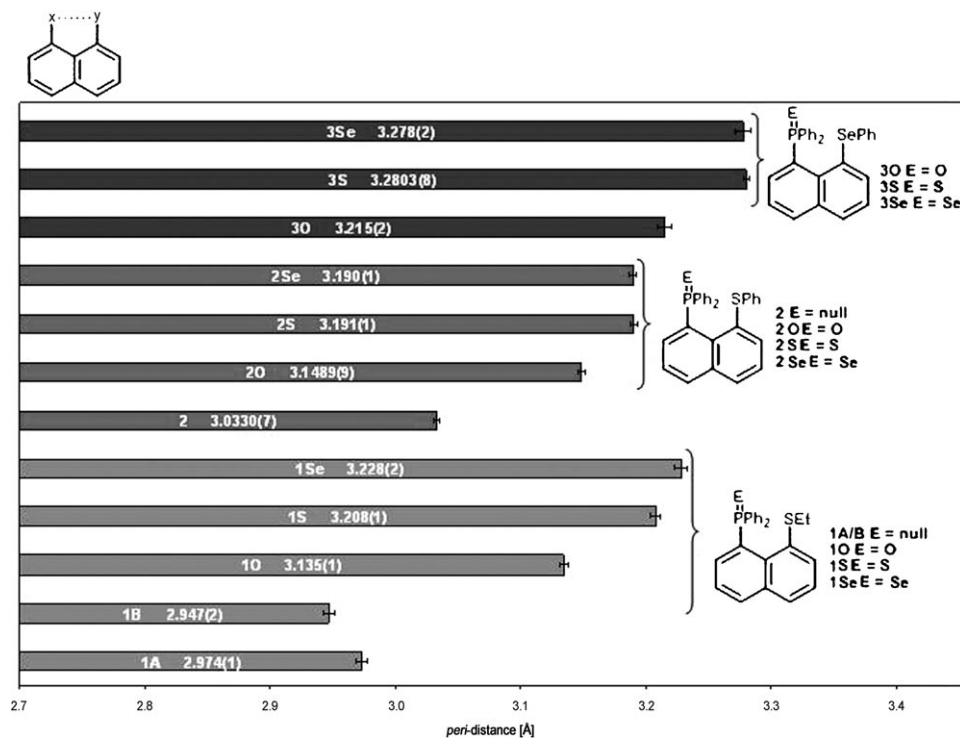


Figure 5. Comparison of the *peri* distances of phosphines **1–3** and their P^V chalcogenides.

increase in the length of the *peri* distance by 4 to 8% upon the exchange of the phosphorus lone pair for a chalcogen atom. These short non-bonded *peri* distances indicate the possible existence of weak intramolecular interactions.^[27]

The increased congestion of the *peri* space in the P^V chalcogenide derivatives is accompanied by a significantly larger displacement of the *peri* atoms to opposite sides of the naphthalene best plane (0.40–0.74 Å) compared with phosphines **1** and **2** (0.01–0.16 Å; Figure 6). Considerable repulsion of the P–C and E–C bonds is also evident, with positive splay angles (11.9–17.3°) helping to alleviate the *peri*-space crowding (Figure 5).^[22] The aforementioned distortions are insufficient to overcome the steric strain that occurs in the bay region and are thus supplemented by major deformations of the naphthalene geometry. C–C bonds and C–C–C angles are stretched and a buckling of the naphthalene skel-

eton away from planarity takes place. Bond lengths around C(10), closer to the repulsion, are on average longer than those around C(5) (average 1.44 and 1.42 Å, respectively) and C(1)–C(10)–C(9) bond angles splay to a mean 127° away from the ideal geometry observed for C(4)–C(5)–C(6) (average 119°). Central naphthalene ring C–C–C–C torsion angles (4.3–11.6°) illustrate the extent and variation of twisting occurring in the naphthalene framework of the nine chalcogenide derivatives (Figure 6), which are notably less planar compared with the backbones of phosphines **1** and **2** (0.2–3.5°). S–C (1.77–1.83 Å), Se–C (1.92–1.94 Å), P–C (1.80–1.84 Å), P=O (1.48–1.49 Å), P=S (1.96–1.97 Å) and P=Se (2.11–2.12 Å) bond lengths are within the usual ranges ((1.82 ± 0.05), (1.93 ± 0.05), (1.84 ± 0.05), (1.49 ± 0.05), (1.95 ± 0.05), (2.09 ± 0.05) Å, respectively)^[23] in all nine compounds. The P–C lengths are slightly shortened on oxidation from P^{III} in **1** and **2** to P^V in the chalcogenide derivatives.

The molecular structures of **1O**, **1S** and **1Se** are shown in Figure 7. As expected, a general increase in the steric strain is observed if larger atoms occupy the *peri* region. Non-covalent P...S *peri* distances (**1O** 3.1349(13) Å; **1S** 3.2083(14) Å; **1Se** 3.2283(19) Å) are significantly longer than the separation in **1** (2.9737(14) Å (2.9469(15) Å)), and lengthen as the bulk of the atoms bound to phosphorus increases. Nonetheless, all distances are shorter than the sum of the vdW radii for phosphorus and sulfur by 0.37 to 0.47 Å.

The displacement of the *peri* atoms to opposite sides of the best naphthalene plane is significantly greater in the

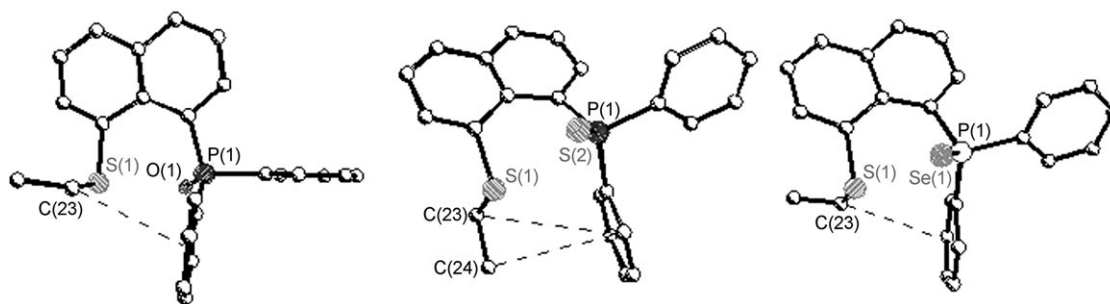


Figure 7. The crystal structures of **1O** (left), **1S** (centre) and **1Se** (right) showing the alignment of the S(ethyl) groups and CH- π interactions.

chalcogenides (0.40–0.74 Å) compared with **1** (0.03–0.16 Å); the greatest out-of-plane distortion was observed in **1S** (–0.62, 0.74 Å). Positive splay angles for **1O** (13.1°) and **1Se** (13.7°) are comparable, which implies that the P–C and S–C bonds are tilted apart to a similar extent to minimise the steric repulsion acting in the *peri* region. Notably, the splay angle of **1S** (11.9°) is smaller and similar to that of phosphine **1** (11.7°). The naphthalene units of **1O** and **1Se** also show similar deviations from planarity, with maximum C–C–C–C torsion angles in the range of 5 to 6°. A major distortion of the naphthalene scaffold is observed in **1S** with the deviation from planarity being more pronounced and larger than any of the chalcogenides reported here; the maximum C–C–C–C torsion angle is 11.6 for C(6)–C(5)–C(10)–C(1) (Figure 6).

As with the structures of compounds **1** and **2**, the conformation and arrangement of the naphthyl rings and ethyl and phenyl groups for the P^V chalcogenides can be categorised relative to the two C(ar)–P(1)–C(ar) planes and the C(ar)–S(1)–C(R) plane (from torsion angles θ and γ , respectively; see Table 5). The torsion angle conformations can be related

to the type A, B, C classification system presented by Nakaniishi et al.,^[25] which can be used to describe the geometry of the molecules (angle θ : axial = type A, equatorial = type B, twist = type C).^[24,25] The torsion angles θ of the naphthalene units in **1O**, **1S** and **1Se** display the same equatorial/axial/axial conformation with respect to the C(ar)–P(1)–C(ar) and C(ar)–S(1)–C(R) planes. This arrangement corresponds to a BA–A–*c* type arrangement (Figure 8);^[24,25] one P–C_{Ph} bond and the S–C_{Et} bond align perpendicular to and on the same side of the naphthyl plane and the remaining P–C_{Ph} bond adopts a position close to/on the plane.^[25] One quasi-linear S \cdots P–C_{Ph} interaction is observed in each compound with angles approaching linearity (174.3, 175.4, 170.9°; Figure 8).

The BA–A–*c* conformation places one phenyl group and the ethyl group attached to S(1) on the same side of the naphthyl plane. The chalcogen bonded to P(1) is thus forced to reside in the *peri* region and in close contact with S(1) (Figure 7). In all cases the chalcogen atom lies below the naphthyl plane, with, as expected, distances from the plane increasing as the size of the atom increases (**1O** –1.7200(51) Å, **1S** –2.019(5) Å, **1Se** –2.3022(69) Å). The non-covalent S(1) \cdots E(2) separations in **1O** (3.033(2) Å), **1S** (3.2951(15) Å) and **1Se** (3.43(1) Å) are shorter than the sum of the vdW radii for the two interacting atoms by 0.27 to 0.31 Å and close enough to suggest possible intramolecular interactions.^[27]

A large number of reported organosulfur compounds contain conformations considerably influenced by intramolecular sulfur-nucleophile interactions;^[27a] such as non-bonded S \cdots O, S \cdots N, S \cdots S and S \cdots π interactions. In these molecules the S \cdots nucleophile distance is significantly shorter than the sum of the sulfur and nucleophile vdW radii.^[27] Although the S(1) \cdots E(2) distances **1O**, **1S** and **1Se** are in the range for in-

Table 5. Torsion angles [°] categorising the naphthyl ring and phenyl/ethyl group conformations in **nO**, **nS** and **nSe** ($n=1-3$).^[a]

	Naphthalene ring conformations			Phenyl ring conformations		
	C(10)–C(1)–P(1)–C(11)	C(10)–C(1)–P(1)–C(17)	C(10)–C(9)–E(1)–C(23)	C(1)–P(1)–C(11)–C(12)	C(1)–P(1)–C(17)–C(18)	C(9)–E(1)–C(23)–C(24)
1O	$\theta_1 = -161.4(1)$; equatorial	$\theta_2 = -89.3(1)$; axial	$\theta_3 = 93.4(1)$; axial	$\gamma_1 = -105.7(1)$; axial	$\gamma_2 = -24.8(1)$; equatorial	$\gamma_3 = 79.1(1)$; axial
1S	$\theta_1 = -158.2(1)$; equatorial	$\theta_2 = 92.6(1)$; axial	$\theta_3 = -89.1(1)$; axial	$\gamma_1 = -98.7(1)$; axial	$\gamma_2 = -160.7(1)$; equatorial	$\gamma_3 = 179.4(1)$; equatorial
1Se	$\theta_1 = -164.9(1)$; equatorial	$\theta_2 = 85.3(1)$; axial	$\theta_3 = -90.9(1)$; axial	$\gamma_1 = 74.2(1)$; axial	$\gamma_2 = 28.9(1)$; equatorial	$\gamma_3 = -67.0(1)$; axial
2O	$\theta_1 = 95.9(1)$; axial	$\theta_2 = 152.7(1)$; equatorial	$\theta_3 = 95.3(1)$; axial	$\gamma_1 = 154.9(1)$; equatorial	$\gamma_2 = 96.5(1)$; axial	$\gamma_3 = -170.0(1)$; equatorial
2S	$\theta_1 = -89.5(1)$; axial	$\theta_2 = 162.0(1)$; equatorial	$\theta_3 = 90.6(1)$; axial	$\gamma_1 = 160.9(1)$; equatorial	$\gamma_2 = -81.4(1)$; axial	$\gamma_3 = 179.5(1)$; equatorial
2Se	$\theta_1 = 162.4(1)$; equatorial	$\theta_2 = -88.3(1)$; axial	$\theta_3 = 92.0(1)$; axial	$\gamma_1 = -77.9(1)$; axial	$\gamma_2 = 161.4(1)$; equatorial	$\gamma_3 = -178.6(1)$; equatorial
3O	$\theta_1 = 146.5(1)$; twist	$\theta_2 = -99.7(1)$; axial	$\theta_3 = 134.5(1)$; twist	$\gamma_1 = -86.3(1)$; axial	$\gamma_2 = -7.2(1)$; equatorial	$\gamma_3 = -56.1(1)$; twist
3S	$\theta_1 = 162.4(1)$; equatorial	$\theta_2 = -88.8(1)$; axial	$\theta_3 = 91.7(1)$; axial	$\gamma_1 = -79.4(1)$; axial	$\gamma_2 = 164.2(1)$; equatorial	$\gamma_3 = -176.5(1)$; equatorial
3Se	$\theta_1 = 162.9(1)$; equatorial	$\theta_2 = -88.5(1)$; axial	$\theta_3 = 93.6(1)$; axial	$\gamma_1 = 102.5(1)$; axial	$\gamma_2 = -20.4(1)$; equatorial	$\gamma_3 = -2.2(1)$; equatorial

[a] Definitions: axial: perpendicular to C(ar)–Z–C(R) plane; equatorial: coplanar with C(ar)–Z–C(R) plane; twist: intermediate between equatorial and axial.

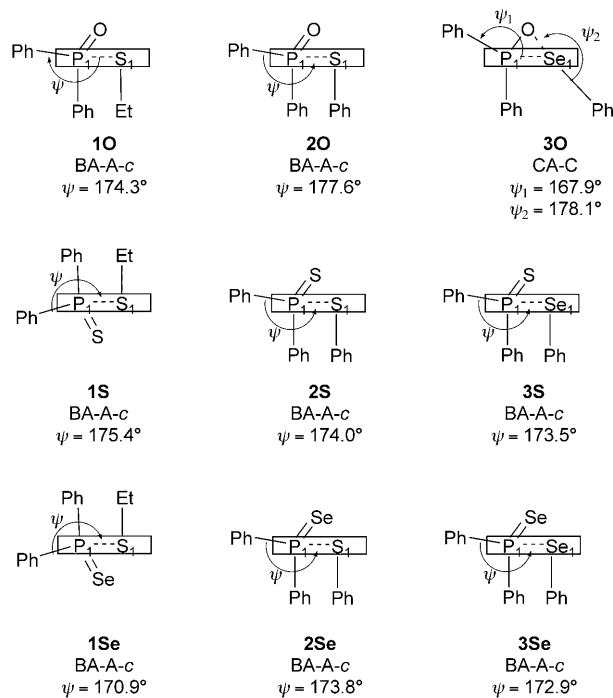


Figure 8. The orientation of the phenyl and ethyl groups, the structure type and the quasi-linear arrangements of **nO**, **nS** and **nSe** ($n=1-3$).^[25]

tramolecular interaction, a rotation around the C(1)–P(1) bond would bring the two interacting moieties in closer contact and produce shorter separations in line with known non-bonded interaction values.^[27] If an S(1)⋯E(2) interaction takes place it is likely to be weak and not the fundamental influence on the geometry of the molecules.

Although all three chalcogenides adopt the BA-A-*c* conformation, torsion angles γ , show that the phenyl and ethyl moieties arranged *cis* to the naphthyl plane adopt different orientations and, therefore, interact slightly differently.^[24,25] In **1O** and **1Se** the ethyl group aligns with an axial conformation ($\gamma_3=79.1(1)^\circ$; $\gamma_3=-67.0(1)^\circ$) in which the C(23)–C(24) bond points directly away from the closest phenyl ring (Figure 7). The C(23)⋯centroid distance is small enough to suggest a possible CH– π interaction for both **1O** (C(23)⋯Cg(17–22) 3.644(1) Å) and **1Se** (C(23)⋯Cg(17–23) 3.578(1) Å).^[28] These are weak non-covalent attractive “hydrogen-bond-type” interactions between soft acids (CH) and soft bases (π system), which have previously been shown to be important in self-assembly and molecular recognition processes and in determining conformations, selectivities of reactions and crystal structures.^[28] The ethyl group in **1S** aligns with an equatorial conformation ($\gamma_3=179.4(1)^\circ$), and the C(23)–C(24) bond lies parallel to the phenyl ring and close enough

to envisage CH– π interactions (C(23)⋯Cg(17–23) 4.041(1) Å, C(24)⋯Cg(17–23) 3.790(1) Å; Figure 7).^[28] CH⋯ π hydrogen-bond lengths are displayed in Table 6.

Table 6. Non-bonded (hydrogen bond) intramolecular ethyl– π interactions [Å] and angles [°] for chalcogenides **1O**, **1S** and **1Se**.^[a]

	D–H⋯A	H⋯A	D⋯A	D–H⋯A
1O	C(23)–H(23a)⋯Cg(17–23)	3.09(1)	3.64(1)	117.2(1)
	C(23)–H(23b)⋯Cg(17–23)	3.59(1)	3.64(1)	85.4(1)
1S	C(23)–H(23b)⋯Cg(17–23)	3.83(1)	4.04(1)	94.9(1)
	C(24)–H(24b)⋯Cg(17–23)	2.90(1)	3.79(1)	151.5(1)
1Se	C(23)–H(23a)⋯Cg(17–23)	3.42(1)	3.58(1)	91.0(1)
	C(23)–H(23b)⋯Cg(17–23)	3.16(1)	3.58(1)	106.8(1)

[a] Cg(17–23) is the centroid of atoms C(17)–C(22). All CH bonds have been refined to 0.99(1) Å.

The molecular structures of **2O**, **2S** and **2Se** are shown in Figure 9. As expected, the P and S *peri* atoms are forced to lie further apart in these chalcogenides than in phosphine **2** (3.0339(13) Å), with longer intramolecular *peri* distances accommodating the greater steric congestion of the *peri* region. Oxide **2O** (3.1489(9) Å) and sulfide **2S** (3.1909(1) Å) have lengths comparable to their S(ethyl) counterparts, whereas the separation of the *peri* atoms in selenide **2Se** (3.190(1) Å) is shorter than expected and simi-

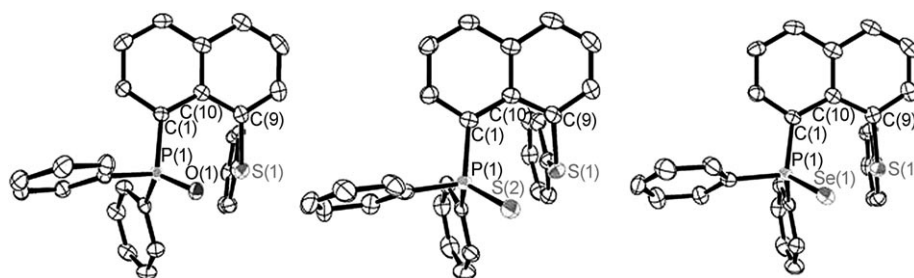


Figure 9. The crystal structures of phosphorus(V) chalcogenides **2O** (left), **2S** (centre) and **2Se** (right).

lar in size to the sulfide compounds. The displacement of the *peri*-atoms to opposite sides of the least-squares naphthalene plane (0.43–0.63 Å) is comparable throughout the series of compounds and more pronounced than in phosphine **2** (0.01, 0.13 Å). Corresponding splay angles of 13.7 and 14.1° imply that distortion of the bay area geometry is also similar for **2S** and **2Se**, whereas a smaller but still positive splay angle of 12.4° is observed in **2O**. Compound **2O** exhibits the largest amount of buckling within the naphthalene unit, with central naphthalene ring C–C–C–C torsion angles in the range of 8 to 10°. The naphthalene scaffold sees a smaller deviation from planarity in **2S** and **2Se** ($\approx 5-7^\circ$).

The S(phenyl) chalcogenides display BA-A-*c* type structures similar those of the S(ethyl) derivatives, with the naphthalene units adopting equatorial/axial/axial conformations with respect to the C(ar)–P(1)–C(ar) and C(ar)–S(1)–C(R) planes (Figure 8).^[24,25] One quasi-linear S⋯P–C_{Ph} interaction

with angles of 177.6, 174.0, and 173.8° is observed in each compound (Figure 8). The *cis* orientation of phenyl groups again forces the extra chalcogen atom to reside in the *peri* region and in close contact with S(1); in all cases lying above the naphthyl plane with distances from the plane increasing as the size of the atom increases (**2O** 1.6231(46) Å, **2S** 2.1977(43) Å, **2Se** 2.3457(51) Å; Figure 9). Non-bonded interatomic S(1)⋯E(2) distances in **2O** (2.9612(17) Å), **2S** (3.3142(11) Å) and **2Se** (3.3974(10) Å) are comparable to those found for the S(ethyl) derivatives and shorter than the sum of the vdW radii for the two interacting atoms by 9 to 12%.^[21] This once again suggests that the non-bonded distance is close enough for possible weak intramolecular interactions to occur.^[27]

Torsion angles (γ) show that the phenyl rings arranged *cis* to the naphthyl plane adopt equatorial conformations in all three compounds and thus overlap in a slipped packing arrangement.^[26] However, variations in the twist of the phenyl groups are observed. A greater overlap of the rings is found in **2S** ($\gamma_1=160.9(1)^\circ$, $\gamma_3=179.5(1)^\circ$) and **2Se** ($\gamma_2=161.4(1)^\circ$, $\gamma_3=178.6(1)^\circ$), which adopt a parallel alignment similar to the face-to-face offset arrangement (Figure 10).^[24,26] The

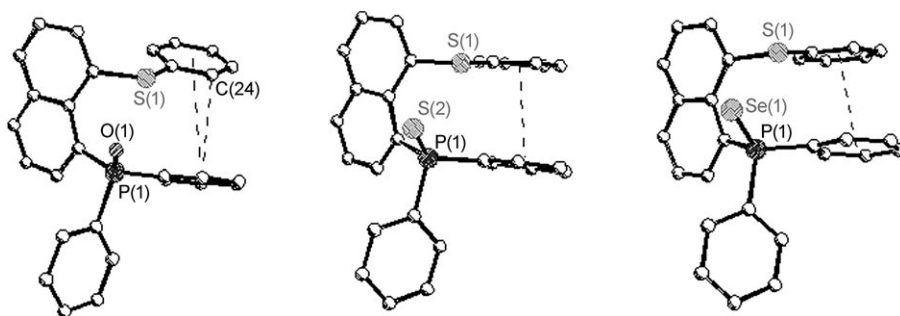


Figure 10. The crystal structures of **2O** (left), **2S** (centre) and **2Se** (right) showing the orientation and overlap of the phenyl rings.

phenyl rings in **2O** ($\gamma_1=154.9(1)^\circ$, $\gamma_3=170.0(1)^\circ$) twist in towards one another and thus do not align parallel (Figure 10). The distances between the two interacting centroids (Cg(17–22)⋯Cg(23–28)) for all three compounds (**2O** 4.397(1) Å, **2S** 3.955(1) Å, **2Se** 3.995(1) Å) is longer than the range for typical centroid–centroid π stacking (3.3–3.8 Å),^[26] and no π – π stacking is observed.^[26]

The molecular structures of **3O**, **3S** and **3Se** are shown in Figure 11. With the substitution of the larger Se(phenyl) moiety at the C(9) *peri* position, congestion of the *peri* region would be expected to increase compared with chalcogenides containing the S(ethyl) and the S(phenyl) functional groups. Greater deformation of the

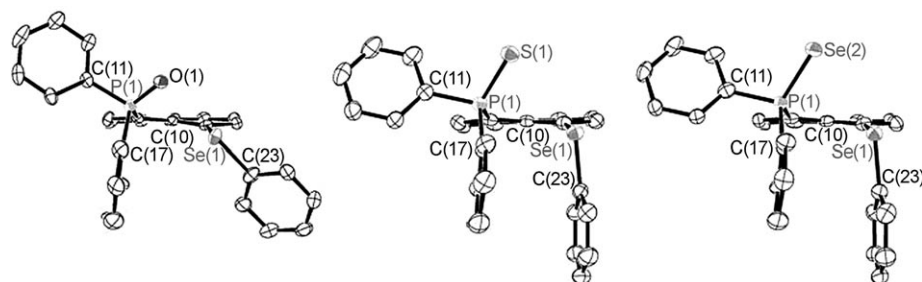


Figure 11. The crystal structures of phosphorus(V) chalcogenides **3O** (left), **3S** (centre) and **3Se** (right) showing the difference between the CA-C and BA-A structures and the overlap of phenyl rings.

naphthalene geometry is observed in **3O**, **3S** and **3Se** than in analogous sulfur compounds to alleviate the extra steric strain. An increase in the distortion is also observed within the group as the size of chalcogen bonded to P(1) increases.

Phosphorus and selenium functional groups lie in close proximity to each other, with non-bonded *peri* distances in **3O** (3.215(2) Å), **3S** (3.2803(8) Å) and **3Se** (3.278(2) Å) showing a general increase as the size of the chalcogen at P(1) increases. The *peri* separation in selenide **3Se**, like its sulfur analogue **2Se**, is shorter than expected and similar in size to the separation in sulfide **3S**. Unsurprisingly, the *peri* gaps observed for the Se(phenyl) compounds are notably larger than those for analogous chalcogenides that contain sulfur functional groups at the C(9) position. Nonetheless, all P⋯Se separations are shorter than the sum of the vdW radii for phosphorus and selenium (3.70 Å)^[21] by 0.42–0.49 Å.

A similar displacement of the *peri* atoms to either side of the naphthalene least-squares plane is observed throughout the series of Se(phenyl) chalcogenides (0.40–0.60 Å) and comparable to the out-of-plane distortion for the S(phenyl) analogues (0.43–0.63 Å). However, distortion within the

naphthyl plane is much more pronounced in the selenium compounds and increases significantly from oxide **3O** to selenide **3Se**. Large and positive splay angles of 15.5 (**3O**), 16.8 (**3S**) and 17.3° (**3Se**) illustrate a major tilt of the *peri* bonds in opposite directions to reduce the greater steric repulsion acting between the heavy atoms in the bay region. The displacement of the phosphorus and selenium substituents within and out of the plane is accompanied by a distortion of the usually

planar and rigid C₁₀ unit by a twist into a non-planar conformation. The deformation of the naphthalene skeleton in selenium compounds **3O**, **3S** and **3Se** corresponds to the distortion occurring in the S(phenyl) chalcogenides **2O**, **2S** and **2Se**. Oxide **3O** shows the greatest deviation from planarity with central naphthalene ring torsion angles of 6 to 10°,

whereas a smaller contortion of the scaffold is observed for **3S** and **3Se** ($\approx 4\text{--}6^\circ$). In fact, the naphthalene unit of **3Se** is the most planar of the chalcogenides reported here (Figure 6).

Compounds **3S** and **3Se** adopt the same BA-A-*c* type structure as the S(ethyl) and S(phenyl) chalcogenides, in which the conformation of the naphthalene unit is equatorial/axial/axial with respect to the C(ar)-P(1)-C(ar) and C(ar)-S(1)-C(R) planes (Figures 8 and 13).^[24,25] One quasi-linear Se...P-C_{Ph} interaction exists in **3S** and **3Se**, with angles 173.5 and 172.9°, respectively (Figure 8). Oxide **3O** adopts a similar but notably different structural arrangement to the other chalcogenides reported here (Figure 11). Relative to the C(ar)-P(1)-C(ar) and C(ar)-S(1)-C(R) planes, the naphthalene unit now assumes a twist/axial/twist arrangement ($\theta_1 = 146.5(1)^\circ$, $\theta_2 = -99.7(1)^\circ$, $\theta_3 = 134.5(1)^\circ$) that corresponds to a CA-C type structure (Figure 8).^[24,25] The P-C_{Ph} and Se-C_{Ph} bonds, which align along and perpendicular to the naphthyl plane, respectively, in **3O** and lie at an intermediate angle ($\approx 45^\circ$; Figure 11). With this conformation, the linearity of the Se...P-C_{Ph} interaction in **3O** is reduced (167.9°); however, the twist conformation of the Se(phenyl) moiety promotes the formation of a quasi-linear O...Se-C_{Ph} arrangement (178.1°; Figure 8).^[24,25]

Both the BA-A and CA-C type structures position the chalcogen atom bonded to P(1) in the *peri*-region and in close contact with Se(1). E(2)...Se(1) non-bonded interatomic distances in **3O** (2.770(3) Å), **3S** (3.3490(7) Å) and **3Se** (3.4217(8) Å) increase across the series with separations shorter than the sum of the vdW radii of the interacting atoms in all cases.^[21] The O(1)...Se(1) contact in **3O** is notably close, with a distance that is 19% shorter than the vdW sum of oxygen and selenium. This distance is shorter than expected when compared with the E(2)...E(1) distances observed in the remaining chalcogenides reported herein, which contain relatively longer distances (7–11% of the vdW sum). These distances are short enough for the existence of non-bonded weak intramolecular interactions to occur.^[27]

The parallel alignment of phenyl groups arranged *cis* to the naphthyl plane in **3S** and **3Se** is confirmed by torsion angles (γ), which show that both rings adopt equatorial conformations (**3S**: $\gamma_2 = 164.2(1)^\circ$, $\gamma_3 = -176.5(1)^\circ$; **3Se**: $\gamma_2 = -20.4(1)^\circ$, $\gamma_3 = -2.2(1)^\circ$). Although the rings adopt a parallel displacement, the distance between the two interacting centroids (Cg(17–22)...Cg(23–28)) is longer than the range for typical centroid-centroid π interactions (3.3–3.8 Å)^[26] for both **3S** (4.034(1) Å) and **3Se** (4.075(1) Å), so no π - π stacking is envisaged (Figure 11).

Compound **3** and its oxide **3O** were previously reported by Nakanishi et al. while they were studying non-bonded lone-pair interactions in *peri*-substituted naphthalenes.^[19] Quantum-chemical calculations performed on optimised structures of models **A** and **B** (Figure 12) were used to reproduce the structure around P and Se in **3O** and to investigate the effect of lone-pair orbitals in the non-bonded P...Se interaction on the structure of the molecule. Based on their

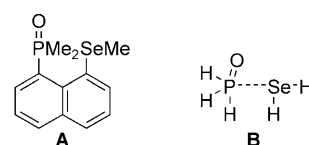


Figure 12. Ab initio MO calculations were performed on models **A** and **B** by Nakanishi et al.^[19]

MO calculations, the 3c–4e type interaction was reported to induce a linear O...Se–H alignment in the models, and the structure of **3O** with its linear O...Se–C arrangement was, therefore, reported to originate from the 3c–4e type interaction of the linear O...Se–C atoms.^[19]

To try and assess the possibility of direct P...Se and E(2)...Se bonding interactions that would indicate an onset of 3c–4e bonding, density functional theory computations were performed for derivatives **2O**, **3O**, **3S** and **3Se** at the B3LYP/6-31+G* level. For each compound, both linear-type arrangements (E(2)...E(1)–C and E(1)...P–C) were evaluated (Figure 13). The Wiberg bond index (WBI),^[29] which measures the covalent bond order, was calculated for each linear arrangement, both for the structures found in the solid and for the minima resulting from full geometry optimisations in the gas phase. WBI values of 0.02 to 0.04 are obtained throughout, which indicates a very minor interaction between non-bonded atoms in these compounds. For comparison, the fully covalent S–S single bond in naphtho-[1,8-*cd*][1,2]dithiole has a WBI of 0.99 at the same level. For **3S** and **3Se**, the aromatic π stacking between the phenyl groups at P and the chalcogen that is found in the solid is lost upon optimisation (due to the missing dispersion interaction at that level), but this only slightly affects the computed WBIs. When the equatorial Ph group on Se(1) in 1,8-bis(phenylselanyl)naphthalene is replaced with Br, Se–Se distances as short as 2.516 Å have been observed.^[30] A B3LYP computation for the latter molecule from the X-ray structure affords a WBI of 0.55, which suggests a large extent of 3c–4e bonding in this case. Judging from the refined phosphorus–chalcogen and chalcogen–chalcogen distances, none of the species in the present study comes close to such a bonding situation.

Further calculations were performed on the radical cations of chalcogenides **2O**, **3O**, **3S** and **3Se** (Figure 13). Although the WBI values for the phosphorus–chalcogen interactions showed little change, the values for the E(2)...Se(1) interaction in the radical cations of selenium compounds **3O**, **3S**, and **3Se** increased to between 0.14 and 0.19, which indicates a greater interaction compared with the neutral species. This increase is a consequence of the nature of the HOMO in the latter species, which consists essentially of p orbitals on E(2) and Se(1) in an antibonding combination (see Figure 14 for **3Se**). Because MOs with the corresponding bonding combination are lower in energy, removal of an electron from the HOMO increases the net bond order between these atoms. No similar increase was observed for the O(1)...S(1) interaction in **2O** upon oxidation.

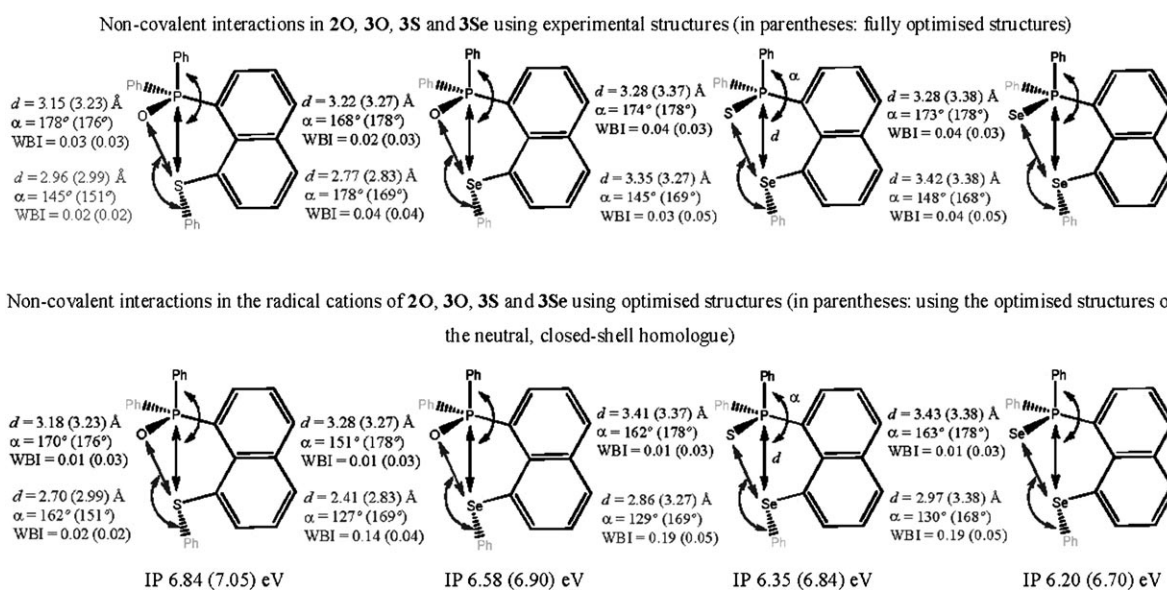


Figure 13. DFT calculations performed on chalcogenides **2O**, **3O**, **3S** and **3Se** and their radical cations (B3LYP/6-31+G* level).

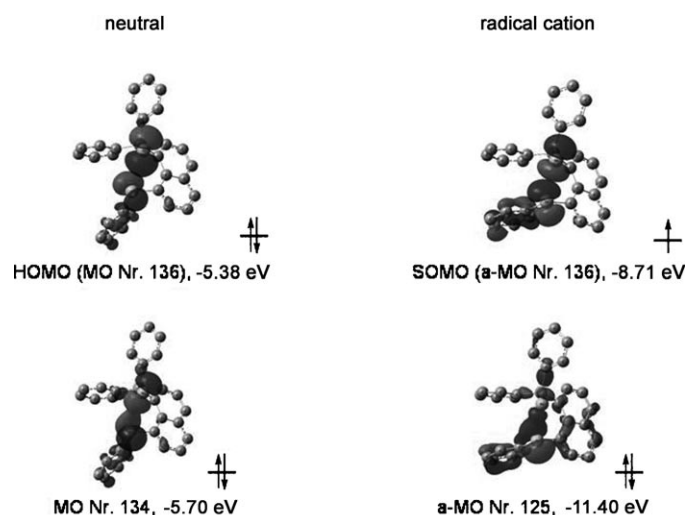


Figure 14. Selected MOs of the neutral and radical cation species of **3Se** (B3LYP level) showing bonding (bottom) and antibonding (top) combinations of p orbitals on the Se atoms.

For each of the radical cations, the adiabatic and vertical ionisation potentials were calculated, and the obtained values of 6.84–6.20 and 7.05–6.70 eV, respectively (Figure 13), are comparable to those of the known compound naphtho[1,8-*cd*][1,2]dithiole, which has adiabatic and vertical IP values of 7.82 and 8.03 eV, respectively, computed at the same level. From previous unpublished work from the Woollins group it was shown that naphtho[1,8-*cd*]-[1,2]dithiole can undergo one-electron oxidation and forms crystals of $[\text{C}_{10}\text{H}_6\text{S}_2]^+[\text{BF}_4]^-$ using electrocrystallisation

techniques.^[31] Judging from the computed IP values, the four chalcogenides **2O**, **3O**, **3S** and **3Se**, could exhibit similar electrochemical reactivity to naphtho[1,8-*cd*][1,2]dithiole and may be able to form charge transfer compounds.

Conclusion

Phosphorus–chalcogen naphthalenes **1–3** have been prepared by using standard halogen–lithium exchange reactions of 1-halo-8-(alkylchalcogeno)naphthalene derivatives,^[5] followed by treatment with dichlorodiphenylphosphine. Compounds **1–3** react to form a complete series of P^{V} chalcogenides that exhibit greater steric crowding due to the presence of an extra chalcogen atom in the *peri* region and by inference a greater deformation of the naphthalene geometry. The presence of quasi-linear three-body fragments in the chalcogenides ($\text{O}\cdots\text{Se}-\text{C}_{\text{Ph}}/\text{E}\cdots\text{P}-\text{C}_{\text{Ph}}$; $171\text{--}178^\circ$) accompanied by $\text{O}\cdots\text{Se}$ and $\text{E}\cdots\text{P}$ distances shorter than the sum of the vdW radii suggests attractive 3–4e interactions could be operating. To try and assess the possibility of direct $\text{O}\cdots\text{Se}/\text{E}\cdots\text{P}$ bonding interactions that would indicate an onset of 3c–4e bonding in the chalcogenides, density functional theory computations were performed for derivatives **2O**, **3O**, **3S** and **3Se**. Judging from the WBI^[29] values of 0.02 to 0.04, none of the species in the present study comes close to such a bonding situation and instead steric effects dominate the overall geometry of the molecules.

We have recently reported a preliminary study of the coordination chemistry of the novel phosphorus–sulfur ligand **2**^[18] to show the potential of these ligands towards specific metal coordination. The difference in electronic properties between donor atoms (P,S) and (P,Se) gives these compounds added value as hemilabile ligands^[14] and the pres-

ence of the extra chalcogen atom in the chalcogenides adds the potential to form extended seven-membered chelate complexes upon coordination with transition metals.^[32]

Experimental Section

All experiments were carried out under an oxygen- and moisture-free nitrogen atmosphere by using standard Schlenk techniques and glassware. Reagents were obtained from commercial sources and used as received. Dry solvents were collected from a MBraun solvent system. 1-Halo-8-(phenylchalcogeno)naphthalene derivatives^[5] were prepared from 1,8-dibromonaphthalene **11**^[33] and 1,8-diiodonaphthalene **12**^[34]. Elemental analyses were performed by the University of St Andrews School of Chemistry Microanalysis Service. IR spectra were recorded as KBr discs in the range of 4000–300 cm⁻¹ on a Perkin–Elmer System 2000 Fourier transform spectrometer. ¹H and ¹³C NMR spectra were recorded by using a Jeol GSX 270 MHz spectrometer with $\delta(\text{H})$ and $\delta(\text{C})$ referenced to external tetramethylsilane. ³¹P and ⁷⁷Se NMR spectra were recorded by using a Jeol GSX 270 MHz spectrometer with $\delta(\text{P})$ and $\delta(\text{Se})$ referenced to external phosphoric acid and dimethylselenide, respectively. Assignments of ¹³C and ¹H NMR spectra were made with the help of H–H COSY and HSQC experiments. All measurements were performed at 25 °C. All values reported for NMR spectroscopy are in parts per million (ppm). Coupling constants (*J*) are given in Hertz (Hz). Mass spectrometry was performed by the University of St Andrews Mass Spectrometry Service. Electron impact mass spectrometry (EIMS) and chemical ionisation mass spectrometry (CIMS) were carried out by using a Micromass GCT orthogonal acceleration time-of-flight mass spectrometer. Electrospray mass spectrometry (ESMS) was carried out by using a Micromass LCT orthogonal accelerator time-of-flight mass spectrometer.

(8-Ethylsulfanylnaphth-1-yl)diphenylphosphine (Nap[PPH₂][SEt]; **1**)

Synthesis of 1 from 4Br: A solution of *n*-butyllithium (2.5 M) in hexane (0.5 mL, 1.1 mmol) was added dropwise to a freshly prepared solution of 1-bromo-8-(ethylsulfanyl)naphthalene (0.3 g, 1.1 mmol) in diethyl ether (10 mL) at –10–0 °C (salted ice bath). The bright mixture was stirred for 2 h at this temperature, after which chlorodiphenylphosphine (0.24 g, 0.2 mL, 1.1 mmol) was added slowly, initially colouring the reaction mixture a bright yellow that became pale yellow once the addition was complete. Stirring was continued for a further 2 h at –10–0 °C, then the mixture was allowed to warm to RT. The solvent was removed in vacuo and hexane (40 mL) was added to precipitate out unwanted salts. The solution was filtered under nitrogen and the solvent removed in vacuo, then the obtained yellow solid was recrystallised from toluene to give the title product as colourless crystals (0.2 g, 40%). ¹H NMR (270 MHz, CDCl₃, 25 °C, TMS): δ = 7.82–7.63 (m, 5H; nap 4,5,7-H, 2 × PPh₂ 4-H), 7.39–7.30 (m, 2H; nap 3,6-H), 7.28–7.10 (m, 9H; nap 2-H, 2 × PPh₂ 2,3,5,6-H), 2.64 (q, ³J(H,H) = 7.4 Hz, 2H; SCH₂), 0.91 ppm (t, ³J(H,H) = 7.4 Hz, 3H; SCH₂CH₃); ¹³C NMR (67.9 MHz, CDCl₃, 25 °C, TMS): δ = 137.0 (s), 136.0 (s), 134.1 (d, *J*(C,P) = 19.7 Hz), 130.8 (s), 130.0 (s), 128.6 (s), 128.4 (d, *J*(C,P) = 7.2 Hz), 125.6 (d, *J*(C,P) = 5.8 Hz), 125.5 (s), 35.2 (s; CH₂), 13.3 ppm (s; CH₃); ³¹P NMR (109.4 MHz, CDCl₃, 25 °C, H₃PO₄): δ = –5.26 ppm; IR (KBr disk): $\tilde{\nu}_{\text{max}}$ = 3430 br, 3054 s, 2919 s, 2227 s, 1587 s, 1480 s, 1434 vs, 1308 s, 1261 s, 1185 s, 1096 vs, 1021 s, 997 s, 910 s, 820 s, 725 vs, 690 vs, 528 vs, 321 s, 294 cm⁻¹ s; MS (ES⁺): *m/z* (%): 411.18 (100) [M+K]⁺; elemental analysis calcd (%) for C₂₄H₂₁PS: C 74.2, H 5.5; found: C 74.5, H 6.1.

Synthesis of 1 from 4I: A solution of *n*-butyllithium (2.5 M) in hexane (0.4 mL, 1.0 mmol) was added dropwise to a freshly prepared solution of 1-iodo-8-(ethylsulfanyl)naphthalene (0.3 g, 1.0 mmol) in diethyl ether (10 mL) at –10–0 °C (salted ice bath). The bright mixture was stirred for 2 h at this temperature, after which chlorodiphenylphosphine (0.23 g, 0.2 mL, 1.0 mmol) was added slowly, initially colouring the reaction mixture a bright yellow that became pale yellow once the addition was complete. Stirring was continued for a further 2 h at –10–0 °C, then the mixture was allowed to warm to RT. The solvent was removed in vacuo and hexane (40 mL) was added to precipitate out unwanted salts. The solu-

tion was filtered under nitrogen and the solvent removed in vacuo (0.2 g, 52%). The product was identified by using ¹H and ³¹P NMR spectroscopy.

(8-Ethylsulfanylnaphth-1-yl)diphenylphosphine oxide (Nap[O:PPH₂][SEt]; **1O):** (8-Ethylsulfanylnaphth-1-yl)diphenylphosphine **3** readily oxidised in contact with the atmosphere to give (8-ethylsulfanylnaphth-1-yl)diphenylphosphine oxide **16** as a white solid with 100% conversion, as monitored by ³¹P NMR spectroscopy. Colourless crystals were obtained by diffusion of pentane into a saturated solution of the product in dichloromethane. ¹H NMR (270 MHz, CDCl₃, 25 °C, TMS): δ = 7.92 (d, ³J(H,H) = 8.2 Hz, 1H; nap 4-H), 7.82–7.76 (m, 2H; nap 5,7-H), 7.59–7.51 (m, 4H; 2 × PPh₂ 2,6-H), 7.51–7.44 (m, 1H; nap 2-H), 7.44–7.30 (m, 7H; nap 6-H, 2 × PPh₂ 3–5-H), 7.28–7.22 (m, 1H; nap 3-H), 2.32 (q, ³J(H,H) = 7.4 Hz, 2H; SCH₂), 0.65 ppm (t, ³J(H,H) = 7.4 Hz, 3H; SCH₂CH₃); ¹³C NMR (67.9 MHz, CDCl₃, 25 °C, TMS): δ = 138.7 (d, *J*(C,P) = 12.5 Hz), 137.7 (s), 134.4 (d, *J*(C,P) = 3.1 Hz), 131.3 (d, *J*(C,P) = 9.3 Hz), 130.7 (d, *J*(C,P) = 2.1 Hz), 128.4 (d, *J*(C,P) = 12.4 Hz), 126.5 (s), 124.1 (d, *J*(C,P) = 14.6 Hz), 33.9 (s; CH₂), 13.5 ppm (s; CH₃); ³¹P NMR (109.4 MHz, CDCl₃, 25 °C, H₃PO₄): δ = 36.34 ppm; IR (KBr disk): $\tilde{\nu}_{\text{max}}$ = 3406 w, 3050 w, 2924 w, 2360 vs, 2341 vs, 1815 w, 1765 w, 1726 w, 1710 w, 1961 w, 1658 s, 1641 s, 1592 vs, 1548 s, 1536 s, 1482 s, 1438 vs, 1316 s, 1187 vs, 1112 s, 1096 s, 994 s, 885 s, 818 vs, 761 vs, 730 s, 715 w, 690 s, 562 vs, 539 vs, 524 s, 507 vs, 434 s, 403 w, 389 w, 363 cm⁻¹ w; MS (ES⁺): *m/z* (%): 411.00 (100) [M+Na]⁺; elemental analysis calcd (%) for C₂₄H₂₁POS: C 74.2, H 5.5; found: C 74.5, H 6.1.

(8-Ethylsulfanylnaphth-1-yl)diphenylphosphine sulfide (Nap[S:PPH₂][SEt]; **1S):** Powdered sulfur (9 mg, 0.27 mmol) was added in small batches to a solution of (8-ethylsulfanylnaphth-1-yl)diphenylphosphine **3** (0.10 g, 0.27 mmol) in toluene (10 mL) at 0 °C. The mixture was stirred for 30 min at 0 °C and then for 2 h at ambient temperature. The resulting cloudy solution was filtered, the solvent was removed in vacuo and the remaining oil was vigorously stirred with hexane (10 mL) overnight, which resulted in a thick suspension. The yellow solid was collected by filtration and the product was obtained as colourless crystals by diffusion of pentane into a saturated solution of the solid in dichloromethane (0.02 g, 72%). ¹H NMR (270 MHz, CDCl₃, 25 °C, TMS): δ = 7.98–7.89 (m, 2H; nap 4,5-H), 7.89–7.65 (m, 5H; nap 7-H, 2 × PPh₂ 2,6-H), 7.54–7.33 (m, 8H; nap 3,6-H, 2 × PPh₂ 3–5-H), 7.32–7.21 (m, 1H; nap 2-H), 2.18–2.04 (m, 2H; SCH₂), 0.54 ppm (t, ³J(H,H) = 7.4 Hz, 3H; SCH₂CH₃); ¹³C NMR (67.9 MHz, CDCl₃, 25 °C, TMS): δ = 138.1 (s), 137.8 (d, *J*(C,P) = 10.4 Hz), 134.0 (d, *J*(C,P) = 3.1 Hz), 131.5 (d, *J*(C,P) = 2.1 Hz), 131.2 (d, *J*(C,P) = 10.4 Hz), 130.5 (d, *J*(C,P) = 2.1 Hz), 130.3 (s), 128.7 (d, *J*(C,P) = 12.4 Hz), 128.4 (d, *J*(C,P) = 12.4 Hz), 126.7 (s), 124.0 (d, *J*(C,P) = 14.5 Hz), 35.2 (s; CH₂), 13.2 ppm (s; CH₃); ³¹P NMR (109.4 MHz, CDCl₃, 25 °C, H₃PO₄): δ = 51.84 ppm; IR (KBr disk): $\tilde{\nu}_{\text{max}}$ = 3048 w, 2957 s, 2923 vs, 2851 s, 1987 w, 1962 w, 1896 w, 1820 w, 1737 w, 1666 w, 1585 w, 1476 w, 1433 s, 1370 w, 1320 w, 1260 s, 1183 w, 1092 s, 1019 w, 991 w, 968 w, 920 w, 880 w, 849 w, 820 vs, 801 vs, 765 s, 746 s, 718 s, 690 s, 645 s, 609 w, 576 w, 546 w, 512 w, 490 w, 442 w, 407 cm⁻¹ s; MS (EI⁺): *m/z* (%): 374.98 (28) [M–Et]⁺, 342.99 (100) [M–SEt]⁺, 188.96 (63) [M–SPPH₂]⁺; elemental analysis calcd (%) for C₂₄H₂₁PS₂: C 71.3, H 5.2; found: C 70.1, H 5.7.

(8-Ethylsulfanylnaphth-1-yl)diphenylphosphine selenide (Nap[Se:PPH₂][SEt]; **1Se):** (8-Ethylsulfanylnaphth-1-yl)diphenylphosphine **3** (0.62 g, 1.5 mmol) and Se (0.12 g, 1.5 mmol) were heated under reflux in toluene (10 mL) for 2 h. The resulting cloudy solution was filtered, the solvent was removed in vacuo and the remaining oil was vigorously stirred with hexane (10 mL) overnight, which resulted in a thick suspension. The yellow solid was collected by filtration and the product was obtained as colourless crystals by diffusion of pentane into a saturated solution of the solid in dichloromethane (0.18 g, 65%). ¹H NMR (270 MHz, CDCl₃, 25 °C, TMS): δ = 7.84–7.82 (m, 2H; nap 4,5-H), 7.81–7.60 (m, 5H; nap 7-H, 2 × PPh₂ 2,6-H), 7.42–7.40 (m, 1H; nap 6-H), 7.40–7.19 (m, 8H; nap 2,3-H, 2 × PPh₂ 3–5-H), 2.09–1.92 (m, 2H; SCH₂), 0.48 ppm (t, ³J(H,H) = 7.4 Hz, 3H; SCH₂CH₃); ¹³C NMR (67.9 MHz, CDCl₃, 25 °C, TMS): δ = 138.3 (s), 137.5 (d, *J*(C,P) = 10.4 Hz), 134.1 (d, *J*(C,P) = 3.1 Hz), 133.4–131.4 (brm), 130.6 (d, *J*(C,P) = 2.0 Hz), 130.4 (s), 128.4 (d, *J*(C,P) = 12.4 Hz), 126.8 (s), 124.0 (d, *J*(C,P) = 13.5 Hz), 35.9 (s; CH₂), 13.8 ppm (s; CH₃); ³¹P NMR (109.4 MHz, CDCl₃, 25 °C, H₃PO₄): δ = 41.92 ppm;

⁷⁷Se NMR (51.5 MHz, CDCl₃, 25 °C, PhSeSePh): $\delta = -172.3$ ppm; IR (KBr disk): $\tilde{\nu}_{\max} = 3047$ w, 2952 w, 2922 s, 2851 w, 2360 vs, 2336 vs, 1475 w, 1435 s, 1318 w, 1247 w, 1180 w, 1096 s, 1088 s, 1023 w, 994 w, 973 w, 917 w, 880 w, 820 s, 764 s, 746 s, 690 vs, 615 w, 587 s, 565 s, 533 s, 508 s, 489 w, 442 w, 409 cm⁻¹ w; MS (EI⁺): m/z (%): 343.07 (100) [M–Se]⁺, 188.99 (15) [M–SePPh₂]⁺; elemental analysis calcd (%) for C₂₈H₂₁PSse: C 63.9, H 4.7; found: C 63.4, H 4.7.

(8-Phenylsulfanylnaphth-1-yl)diphenylphosphine (Nap[PPh₂][SPH]; 2)

Synthesis of 2 from 5Br: A solution of *n*-butyllithium (2.5 M) in hexane (1.3 mL, 3.2 mmol) was added dropwise to a freshly prepared solution of 1-bromo-8-(phenylsulfanyl)naphthalene (1.02 g, 3.2 mmol) in diethyl ether (30 mL) at -10 – 0 °C (salted ice bath). The bright mixture was stirred for 2 h at this temperature, after which chlorodiphenylphosphine (0.71 g, 0.6 mL, 3.2 mmol) was added slowly. The mixture was stirred for a further 2 h at -10 – 0 °C, then allowed to warm to RT. The solvent was removed in vacuo and hexane (40 mL) was added to precipitate out unwanted salts. The solution was filtered under nitrogen and the solvent removed in vacuo to give a crude yellow solid that was recrystallised from hexane to give the product as colourless crystals (0.9 g, 64%). ¹H NMR (270 MHz, CDCl₃, 25 °C, TMS): $\delta = 7.93$ – 7.81 (m, 2H; nap 4,5-H), 7.71 (d, ³J(H,H) = 1.5 Hz, 1H; nap 2-H), 7.45–7.36 (m, 1H; nap 3-H), 7.36–7.28 (m, 1H; nap 6-H), 7.26–7.13 (m, 11H; nap 2-H, 2 × PPh₂ 2–6-H), 7.09–6.97 (m, 3H; SPh 3–5-H), 6.77–6.70 ppm (m, 2H; SPh 2,6-H); ¹³C NMR (67.9 MHz, CDCl₃, 25 °C, TMS): $\delta = 140.0$ (q), 139.8 (q), 137.6 (s), 137.0 (s), 135.6 (q), 134.1 (d, J(C,P) = 19.8 Hz), 132.2 (q), 131.3 (d, J(C,P) = 9.4 Hz), 130.9 (s), 130.6 (s), 128.6 (s), 128.4 (d, J(C,P) = 7.3 Hz), 128.1 (d, J(C,P) = 3.1 Hz), 126.4 (q), 125.9 (s), 125.8 (s), 125.4 ppm (s); ³¹P NMR (109.4 MHz, CDCl₃, 25 °C, H₃PO₄): $\delta = -5.30$ ppm; IR (KBr disk): $\tilde{\nu}_{\max} = 3050$ s, 2963 s, 1949 w, 1884 w, 1828 w, 1579 s, 1544 s, 1472 s, 1432 vs, 1352 w, 1308 w, 1261 vs, 1197 s, 1092 vs, 1021 vs, 864 w, 817 vs, 801 vs, 767 vs, 740 vs, 691 vs, 592 w, 539 w, 499 s, 474 s, 424 w, 387 cm⁻¹ s; MS (ES⁺): m/z (%): 459.20 (100) [M+K]⁺; elemental analysis calcd (%) for C₂₈H₂₁PS: C 79.9, H 5.0; found: C 79.7, H 5.0.

Synthesis of 2 from 5I: A solution of *n*-butyllithium (1.6 M) in hexane (1.9 mL, 3.0 mmol) was added dropwise to a freshly prepared solution of 1-iodo-8-(phenylsulfanyl)naphthalene (1.10 g, 3.0 mmol) in diethyl ether (30 mL) at -10 – 0 °C (salted ice bath). The bright yellow mixture was stirred for 2 h at this temperature, after which chlorodiphenylphosphine (0.67 g, 0.5 mL, 3.0 mmol) was added slowly. The mixture was stirred for a further 2 h at -10 – 0 °C, then allowed to warm to RT. The solvent was removed in vacuo and hexane (40 mL) was added to precipitate out unwanted salts. The solution was filtered under nitrogen and the solvent removed in vacuo to give a crude yellow solid that was recrystallised from hexane (0.9 g, 74%). The product was identified by using ¹H and ³¹P NMR spectroscopy.

(8-Phenylsulfanylnaphth-1-yl)diphenylphosphine oxide (Nap[O:PPh₂][SPH]; 2O):

(8-Phenylsulfanylnaphth-1-yl)diphenylphosphine **19** oxidised in contact with the atmosphere to give (8-phenylsulfanylnaphth-1-yl)diphenylphosphine oxide **21** as a white solid with 100% conversion, as monitored by ³¹P NMR spectroscopy. Colourless crystals were obtained by diffusion of pentane into a saturated solution of the obtained product in dichloromethane. M.p./b.p. 50–52 °C; ¹H NMR (270 MHz, CDCl₃, 25 °C, TMS): $\delta = 7.97$ (d, ³J(H,H) = 8.2 Hz, 1H; nap 4-H), 7.90 (d, ³J(H,H) = 8.1 Hz, 1H; nap 5-H), 7.83 (dd, ³J(H,H) = 7.2 Hz, ⁴J(H,H) = 1.3 Hz, 1H; nap 7-H), 7.52–7.40 (m, 6H; nap 2,6-H, 2 × PPh₂ 2,6-H), 7.32–7.23 (m, 3H; nap 3-H, 2 × PPh₂ 4-H), 7.23–7.15 (m, 4H; 2 × PPh₂ 3,5-H), 6.84–6.72 (m, 3H; SPh 3–5-H), 6.18–6.12 ppm (m, 2H; SPh 2,6-H); ¹³C NMR (67.9 MHz, CDCl₃, 25 °C, TMS): $\delta = 139.8$ (s) 138.4 (d, J(C,P) = 12.4 Hz), 134.2 (d, J(C,P) = 4.1 Hz), 131.2 (d, J(C,P) = 9.3 Hz), 130.6 (d, J(C,P) = 2.1 Hz), 128.2 (s), 128.1 (d, J(C,P) = 3.8 Hz), 127.1 (s), 126.3 (s), 124.6 (s), 124.3 ppm (d, J(C,P) = 14.5 Hz); ³¹P NMR (109.4 MHz, CDCl₃, 25 °C, H₃PO₄): $\delta = 37.01$ ppm; IR (KBr disk): $\tilde{\nu}_{\max} = 3393$ w, 3051 w, 2360 vs, 2339 vs, 1954 w, 1868 w, 1843 w, 1769 w, 1716 w, 1699 w, 1651 w, 1581 w, 1557 w, 1539 w, 1519 w, 1507 w, 1475 s, 1435 vs, 1357 w, 1321 w, 1259 w, 1211 w, 1181 vs, 1153 s, 1111 s, 1097 s, 1067 s, 1024 w, 993 s, 930 w, 886 s, 827 vs, 770 s, 734 vs, 715 s, 689 vs, 632 w, 614 w, 587 w, 563 vs, 540 vs, 507 s, 455 s, 419 cm⁻¹ w; MS (CI⁺): m/z (%): 437.12 (100) [M+H]⁺, 327.09

(32) [M–SPh]⁺; elemental analysis calcd (%) for C₂₈H₂₁PSO: C 77.0, H 4.9; found: C 77.7, H 5.0.

(8-Phenylsulfanylnaphth-1-yl)diphenylphosphine sulfide (Nap[S:PPh₂][SPH]; 2S): Powdered sulfur (18.2 mg, 0.569 mmol) was added in small batches to a solution of (8-phenylsulfanylnaphth-1-yl)diphenylphosphine **19** (0.239 g, 0.569 mmol) in toluene (10 mL) at 0 °C. The mixture was stirred for 30 min at 0 °C and then for another 2 h at ambient temperature. The resulting cloudy solution was filtered, the solvent was removed in vacuo and the remaining oil was vigorously stirred with hexane (10 mL) overnight, which resulted in a thick suspension. The yellow solid was collected by filtration and the product was obtained as colourless crystal by diffusion of pentane into a saturated solution of the solid in dichloromethane (0.1 g, 44%). ¹H NMR (270 MHz, CDCl₃, 25 °C, TMS): $\delta = 7.99$ – 7.88 (m, 3H; nap 4,5,7-H), 7.54–7.48 (m, 1H; nap 6-H), 7.32–7.10 (m, 12H; nap 2,3-H, 2 × PPh₂ 2–6-H), 6.81–6.69 (m, 3H; SPh 3–5-H), 5.93–5.87 ppm (m, 2H; SPh 2,6-H); ¹³C NMR (67.9 MHz, CDCl₃, 25 °C, TMS): $\delta = 140.7$ (s), 137.7 (d, J(C,P) = 11.4 Hz), 134.2 (d, J(C,P) = 3.1 Hz), 131.8 (s), 130.5 (s), 128.3 (d, J(C,P) = 12.5 Hz), 128.1 (s), 127.4 (s), 125.3 (s), 124.4 (s), 124.2 ppm (s); ³¹P NMR (109.4 MHz, CDCl₃, 25 °C, H₃PO₄): $\delta = 52.52$ ppm; IR (KBr disk): $\tilde{\nu}_{\max} = 3446$ br, 3062 w, 1966 w, 1847 w, 1579 s, 1543 w, 1473 s, 1430 s, 1381 w, 1357 w, 1321 s, 1302 s, 1272 w, 1199 w, 1177 s, 1150 s, 1089 s, 1022 w, 989 s, 916 w, 882 w, 824 s, 766 vs, 736 vs, 687 s, 642 vs, 611 s, 547 s, 578 w, 547 s, 523 s, 511 vs, 492 s, 468 s, 447 w, 407 cm⁻¹ s; MS (ES⁺): m/z (%): 474.97 (100) [M+Na]⁺; elemental analysis calcd (%) for C₂₈H₂₁PS₂: C 74.3, H 4.7; found: C 73.3, H 4.7.

(8-Phenylsulfanylnaphth-1-yl)diphenylphosphine selenide (Nap[Se:PPh₂][SPH]; 2Se):

(8-Phenylsulfanylnaphth-1-yl)diphenylphosphine **19** (0.23 g, 0.55 mmol) and Se (0.047 g, 0.55 mmol) were heated under reflux in toluene (10 mL) for 2 h. The resulting cloudy solution was filtered, the solvent was removed in vacuo and the remaining oil was vigorously stirred with hexane (10 mL) overnight, which resulted in a thick suspension. The yellow solid was collected by filtration and the product was obtained as yellow crystals by diffusion of pentane into a saturated solution of the crude compound (0.2 g, 85%). ¹H NMR (270 MHz, CDCl₃, 25 °C, TMS): $\delta = 8.00$ – 7.91 (m, 3H; nap 4,5,7-H), 7.56–7.49 (m, 1H; nap 6-H), 7.30–7.10 (m, 12H; nap 2,3-H, 2 × PPh₂ 2–6-H), 6.77–6.67 (m, 3H; SPh 3–5-H), 5.86–5.81 ppm (m, 2H; SPh 2,6-H); ¹³C NMR (67.9 MHz, CDCl₃, 25 °C, TMS): $\delta = 140.7$ (s), 137.3 (d, J(C,P) = 10.4 Hz), 134.2 (d, J(C,P) = 3.2 Hz), 131.9 (s), 130.6 (d, J(C,P) = 3.1 Hz), 128.3 (s), 128.1 (s), 127.6 (s), 125.0 (s), 124.3 (s), 124.2 ppm (s); ³¹P NMR (109.4 MHz, CDCl₃, 25 °C, H₃PO₄): $\delta = 42.46$ ppm (J(P,Se) = 722.4 Hz); ⁷⁷Se NMR (51.5 MHz, CDCl₃, 25 °C, PhSeSePh): $\delta = -341.0$ ppm (d, J(Se,P) = 722.4 Hz); IR (KBr disk): $\tilde{\nu}_{\max} = 2856$ vs, 2395 w, 1718 w, 1646 s, 1542 w, 1461 vs, 1378 w, 1308 w, 1181 w, 1120 w, 973 w, 886 w, 809 s, 722 s, 691 w, 616 w, 562 w, 539 w, 506 cm⁻¹ w; MS (CI⁺): m/z (%): 501.04 (4) [M+H]⁺, 421.12 (75) [M–Se]⁺, 391.02 (12) [M–SPh]⁺, 343.08 (100) [M–SePh]⁺; elemental analysis calcd (%) for C₂₈H₂₁PSse: C 67.3, H 4.2; found: C 65.9, H 4.4.

(8-Phenylselenanylnaphth-1-yl)diphenylphosphine (Nap[PPh₂][SePh]; 3)

Synthesis of 3 from 6Br: A solution of *n*-butyllithium (2.5 M) in hexane (1.1 mL, 2.8 mmol) was added dropwise to a freshly prepared solution of 1-bromo-8-(phenylselenanyl)naphthalene (1.02 g, 2.8 mmol) in diethyl ether (30 mL) at -10 – 0 °C (salted ice bath). The bright yellow mixture was stirred for 2 h at this temperature, after which chlorodiphenylphosphine (0.62 g, 0.5 mL, 2.8 mmol) was added slowly. The mixture was stirred for a further 2 h at -10 – 0 °C, then allowed to warm to RT. The solvent was removed in vacuo and hexane (40 mL) was added to precipitate out unwanted salts. The solution was filtered under nitrogen and the solvent removed in vacuo to give the product as a yellow oil (0.5 g, 40%). ¹H NMR (270 MHz, CDCl₃, 25 °C, TMS): $\delta = 7.76$ (dd, ³J(H,H) = 7.9 Hz, ⁴J(H,H) = 1.5 Hz, 1H; nap 4-H), 7.66 (d, ³J(H,H) = 8.1 Hz, 1H; nap 5-H), 7.52 (dd, ³J(H,H) = 7.4 Hz, ⁴J(H,H) = 1.2 Hz, 1H; nap 7-H), 7.35–7.30 (m, 1H; nap 2-H), 7.30–7.05 ppm (m, 17H; nap 2,3-H, SPh 2–6-H, 2 × PPh₂ 2–6-H); ¹³C NMR (67.9 MHz, CDCl₃, 25 °C, TMS): $\delta = 137.7$ (s), 135.0 (s), 133.9 (d, J(C,P) = 5.2 Hz), 133.7 (s), 131.2 (s), 129.2 (s), 128.9 (s), 128.5 (d, J(C,P) = 6.2 Hz), 128.3 (s), 127.4 (s), 126.1 (s), 125.6 ppm (s); ³¹P NMR (109.4 MHz, CDCl₃, 25 °C, H₃PO₄): $\delta = -12.94$ ppm (J(P,Se) =

386.2.0 Hz); ^{77}Se NMR (51.5 MHz, CDCl_3 , 25 °C, PhSeSePh): $\delta = 439.6$ ppm (d, $J(\text{Se,P}) = 386.2.0$ Hz); IR (KBr disk): $\tilde{\nu}_{\text{max}} = 3853$ w, 3735 w, 3673 w, 3649 w, 3628 w, 3049 w, 2911 w, 2851 w, 2360 vs, 2340 vs, 1734 w, 1699 w, 1651 w, 1558 w, 1541 w, 1474 w, 1433 s, 1310 w, 1259 w, 1193 w, 1153 w, 1088 w, 1021 w, 996 w, 971 w, 911 w, 815 s, 765 s, 739 s, 690 s, 669 s, 538 w, 504 w, 420 w, 397 w, 352 cm^{-1} w; MS (CI^+): m/z (%): 469.06 (65) $[\text{M}+\text{H}]^+$, 391.02 (98) $[\text{M}+\text{H}-\text{Ph}]^+$; elemental analysis calcd (%) for $(\text{C}_{28}\text{H}_{21}\text{PSe})_4\text{CDCl}_3$: C 68.2, H 4.4; found: C 68.4, H 4.6.

Synthesis of 3 from 6I: A solution of *n*-butyllithium (2.5 M) in hexane (0.5 mL, 1.2 mmol) was added dropwise to a freshly prepared solution of 1-iodo-8-(phenylselanyl)naphthalene (0.50 g, 1.2 mmol) in diethyl ether (30 mL) at -10 – 0 °C (salted ice bath). The bright yellow mixture was stirred for 2 h at this temperature, after which chlorodiphenylphosphine (0.27 g, 0.2 mL, 1.2 mmol) was added slowly. The mixture was stirred for a further 2 h at -10 – 0 °C, then allowed to warm to RT. The solvent was removed in vacuo and hexane (40 mL) was added to precipitate out unwanted salts. The solution was filtered under nitrogen and the solvent removed in vacuo to give the product as a yellow oil (0.5 g, 89 %); The product was identified by using ^1H and ^{31}P NMR spectroscopy.

(8-Phenylselanyl)naphth-1-yl)diphenylphosphine oxide (Nap[O:PPh₂]-[SePh]; 3O): (8-Phenylselanyl)naphth-1-yl)diphenylphosphine **32** readily oxidised in contact with the atmosphere to give (8-phenylselanyl)naphth-1-yl)diphenylphosphine oxide **35** as an orange solid with 100 % conversion, as monitored by ^{31}P NMR spectroscopy. The obtained solid was recrystallised by diffusion of pentane into a saturated solution of the compound to give the product as colourless crystals (42%). M.p./b.p. 50–52 °C; ^1H NMR (270 MHz, CDCl_3 , 25 °C, TMS): $\delta = 7.92$ (d, $^3J(\text{H,H}) = 8.2$ Hz, 1H; nap 4-H), 7.88 (d, $^3J(\text{H,H}) = 6.4$ Hz, 1H; nap 5-H), 7.79 (d, $^3J(\text{H,H}) = 8.1$ Hz, 1H; nap 7-H), 7.57–7.48 (m, 4H; $2 \times \text{PPh}_2$ 2,6-H), 7.40–7.32 (m, 3H; nap 2-H, $2 \times \text{PPh}_2$ 4-H), 7.30–7.21 (m, 6H; nap 3,6-H, $2 \times \text{PPh}_2$ 3,5-H), 6.97–6.90 (m, 1H; SPh 4-H), 6.90–6.81 (m, 2H; SPh 3,5-H), 6.59 ppm (d, $^3J(\text{H,H}) = 7.2$ Hz, 2H; SPh 2,6-H); ^{13}C NMR (67.9 MHz, CDCl_3 , 25 °C, TMS): $\delta = 140.3$ (s), 137.6 (q), 137.3 (q), 135.6 (q), 134.3 (s), 131.8 (d, $J(\text{C,P}) = 9.4$ Hz), 131.1 (s), 130.3 (s), 128.6 (s), 128.4 (s), 128.2 (s), 127.1 (s), 126.1 (s), 123.8 ppm (d, $J(\text{C,P}) = 15.5$ Hz); ^{31}P NMR (109.4 MHz, CDCl_3 , 25 °C, H_3PO_4): $\delta = 37.99$ ppm; ^{77}Se NMR (51.5 MHz, CDCl_3 , 25 °C, PhSeSePh): $\delta = 450.4$ ppm; IR (KBr disk): $\tilde{\nu}_{\text{max}} = 3423$ br, 3053 s, 2924 w, 1960 w, 1893 w, 1809 w, 1589 w, 1472 s, 1436 vs, 1314 s, 1176 vs, 1115 vs, 1068 w, 1022 w, 997 w, 981 w, 923 w, 866 w, 821 s, 763 vs, 744 vs, 721 vs, 693 vs, 541 vs, 505 s, 469 w, 447 w, 426 cm^{-1} w; MS (EI^+): m/z (%): 507.02 (100) $[\text{M}+\text{Na}]^+$; elemental analysis calcd (%) for $\text{C}_{28}\text{H}_{21}\text{PSeO}$: C 69.4, H 4.4; found C 68.5, H 4.6.

(8-Phenylselanyl)naphth-1-yl)diphenylphosphine sulfide (Nap[S:PPh₂]-[SePh]; 3S): Powdered sulfur (0.065 g, 0.21 mmol) was added in small batches to a solution of (8-phenylselanyl)naphth-1-yl)diphenylphosphine **32** (0.086 g, 0.21 mmol) in toluene (10 mL) at 0 °C. The mixture was stirred for 30 min at 0 °C and then for 2 h at ambient temperature. The resulting cloudy solution was filtered, the solvent was removed in vacuo and the remaining oil was vigorously stirred with hexane (10 mL) overnight, which resulted in a thick suspension. The yellow solid was collected by filtration and recrystallised by diffusion of pentane into a saturated solution of the compound to give the product as colourless crystals (0.05 g, 54 %). M.p./b.p. 51–53 °C; ^1H NMR (270 MHz, CDCl_3 , 25 °C, TMS): $\delta = 8.12$ (dd, $^3J(\text{H,H}) = 7.1$ Hz, $^4J(\text{H,H}) = 1.4$ Hz, 1H; nap 5-H), 8.00–7.88 (m, 2H; nap 4,7-H), 7.76–7.62 (m, 4H; $2 \times \text{PPh}_2$ 2,6-H), 7.48–7.22 (m, 9H; nap 2,3,6-H, $2 \times \text{PPh}_2$ 3–5-H), 6.97–6.81 (m, 3H; SPh 3–5-H), 6.43–6.35 ppm (m, 2H; SPh 2,6-H); ^{13}C NMR (67.9 MHz, CDCl_3 , 25 °C, TMS): $\delta = 141.2$ (s), 137.9 (s), 134.3 (d, $J(\text{C,P}) = 3.1$ Hz), 132.0 (d, $J(\text{C,P}) = 10.4$ Hz), 131.1 (s), 130.8 (d, $J(\text{C,P}) = 2.0$ Hz), 129.4 (s), 128.5 (d, $J(\text{C,P}) = 4.2$ Hz), 128.3 (s), 127.3 (s), 125.6 (s), 123.9 ppm (s); ^{31}P NMR (109.4 MHz, CDCl_3 , 25 °C, H_3PO_4): $\delta = 51.01$ ppm; ^{77}Se NMR (51.5 MHz, CDCl_3 , 25 °C, PhSeSePh): $\delta = 448.5$ ppm (d, $J(\text{Se,P}) = 19.1$ Hz); IR (KBr disk): $\tilde{\nu}_{\text{max}} = 2925$ vs, 1871 vs, 1574 w, 1474 s, 1434 vs, 1375 w, 1317 w, 1260 s, 1192 w, 1177 w, 1095 s, 1064 w, 1021 s, 994 w, 936 s, 863 w, 797 vs, 769 s, 732 vs, 718 vs, 690 vs, 639 s, 539 s, 509 s, 454 w, 414 cm^{-1} w; MS (CI^+): m/z (%): 501.04 (3) $[\text{M}+\text{H}]^+$, 419.10 (11) $[\text{M}-\text{Ph}]^+$, 345.08 (100) $[\text{M}-\text{Ph}_2]^+$; elemental analysis calcd (%) for $\text{C}_{28}\text{H}_{21}\text{PSSe}$: C 67.2, H 4.2; found C 66.7, H 3.9.

(8-Phenylselanyl)naphth-1-yl)diphenylphosphine selenide (Nap[Se:PPh₂]-[SePh]; 3Se): (8-Phenylselanyl)naphth-1-yl)diphenylphosphine **32** (1.09 g, 2.3 mmol) and Se (0.18 g, 2.3 mmol) were heated under reflux in toluene (20 mL) for 2 h. The resulting cloudy solution was filtered, the solvent was removed in vacuo and the remaining oil was vigorously stirred with hexane (10 mL) overnight, which resulted in a thick suspension. The yellow solid was collected by filtration and recrystallised by diffusion of pentane into a saturated solution of the compound to give the product as yellow crystals (0.8 g, 60 %). ^1H NMR (270 MHz, CDCl_3 , 25 °C, TMS): $\delta = 8.11$ (dd, $^3J(\text{H,H}) = 7.2$ Hz, $^4J(\text{H,H}) = 1.3$ Hz, 1H; nap 5-H), 7.94–7.83 (m, 2H; nap 4,7-H), 7.43–7.14 (m, 13H; nap 2,3,6-H, $2 \times \text{PPh}_2$ 2–6-H), 6.88–6.74 (m, 3H; SPh 3–5-H), 6.27–6.19 ppm (m, 2H; SPh 2,6-H); ^{13}C NMR (67.9 MHz, CDCl_3 , 25 °C, TMS): $\delta = 141.4$ (s), 137.4 (d, $J(\text{C,P}) = 9.4$ Hz), 134.4 (d, $J(\text{C,P}) = 3.1$ Hz), 131.2 (s), 130.8 (d, $J(\text{C,P}) = 3.1$ Hz), 128.8 (s), 128.6 (s), 128.5 (s), 128.4 (s), 128.3 (s), 127.4 (s), 125.5 (s), 123.9 ppm (d, $J(\text{C,P}) = 13.5$ Hz); ^{31}P NMR (109.4 MHz, CDCl_3 , 25 °C, H_3PO_4): $\delta = 40.50$ ppm ($^1J(\text{P,Se}) = 715.3$ Hz, $^4J(\text{P,Se}) = 23.9$ Hz); ^{77}Se NMR (51.5 MHz, CDCl_3 , 25 °C, PhSeSePh): $\delta = 451.4$ (d, $^4J(\text{Se,P}) = 23.9$ Hz), -162.8 ppm (d, $^1J(\text{Se,P}) = 715.3$ Hz); IR (KBr disk): $\tilde{\nu}_{\text{max}} = 2018$ vs, 1954 vs, 1918 vs, 1732 w, 1651 s, 1574 w, 1473 s, 1433 s, 1316 w, 1261 s, 1197 w, 1178 w, 1156 w, 1096 s, 1019 w, 995 w, 978 w, 905 w, 862 w, 824 s, 800 s, 774 w, 765 s, 748 s, 735 s, 686 s, 662 w, 615 w, 583 s, 557 s, 524 s, 505 s, 486 s, 458 s, 443 s, 413 cm^{-1} s; MS (EI^+): m/z (%): 390.01 (5) $[\text{M}-\text{SePh}]^+$, 311.10 (18) $[\text{M}-\text{Se}_2\text{Ph}]^+$, 236.94 (12) $[\text{M}-\text{Ph}_2\text{Se}]^+$, 233.04 (100) $[\text{M}-\text{Se}_2\text{Ph}_2]^+$; elemental analysis calcd (%) for $\text{C}_{28}\text{H}_{21}\text{PSe}_2$: C 61.6, H 3.9; found C 61.4, H 3.3.

Crystal structure analyses: X-ray crystal structures for compounds **1** and **2** were collected at $-180(1)$ °C by using a Rigaku MM007 high brilliance RA generator ($\text{MoK}\alpha$ radiation, confocal optic) and Mercury CCD system. At least a full hemisphere of data was collected by using ω scans. Intensities were corrected for Lorentz, polarisation and absorption. Data for chalcogenide compounds **nO**, **nS**, **nSe** ($n = 1$ – 3) were collected at $-148(1)$ °C by using a Rigaku ACTOR-SM Saturn 724 CCD area detector with confocal optic $\text{MoK}\alpha$ radiation ($\lambda = 0.71073$ Å). The data were corrected for Lorentz, polarisation and absorption. The data for the analysed complexes was collected and processed by using CrystalClear (Rigaku).^[35] The structure was solved by direct methods^[36] and expanded by using Fourier techniques.^[37] The non-hydrogen atoms were refined anisotropically. Hydrogen atoms were refined by using the riding model. All calculations were performed by using the CrystalStructure^[38] crystallographic software package except for refinement, which was performed by using SHELXL-97.^[39] Tables 7, 8 and 9 shows the details of the crystallographic studies. CCDC-737039 (**2**), -776917 (**1**), -776918 (**1O**), -776919 (**1S**), -776920 (**1Se**), -766921 (**2O**), -776922 (**2S**), -776923 (**2Se**), -776924 (**3O**), -776925 (**3S**) and -776926 (**3Se**) contain the supplementary crystallographic data for this paper. These data can be obtained free of charge from The Cambridge Crystallographic Data Centre via www.ccdc.cam.ac.uk/data_request/cif.

Computational details: Geometries were fully optimised in the gas phase at the B3LYP level^[40] by using Curtis and Binning's 962(d) basis^[41] on Se and 6–31+G(d) elsewhere, followed by calculation of the harmonic frequencies to confirm the minimum character of each stationary point and evaluation of WBI values,^[29] obtained in a natural bond orbital analysis.^[42] The optimisations were started from the experimental structures available from X-ray crystallography, for which the WBIs were also calculated. Radical cations were re-optimised from the closed-shell minima by using the unrestricted Kohn–Sham formalism (spin contamination was negligible in all cases). The computations were performed by using the Gaussian 03 suite of programs.^[43]

Table 7. Crystallographic data for compounds **1**, **1O**, **1S** and **1Se**.

	1	1O	1S	1Se
empirical formula	C ₂₄ H ₂₁ PS	C ₂₄ H ₂₁ OPS	C ₂₄ H ₂₁ PS ₂	C ₂₄ H ₂₁ PSSe
<i>M_r</i>	372.44	388.46	404.52	451.42
<i>T</i> [°C]	−180(1)	−148(1)	−148(1)	−148(1)
crystal colour, habit	colourless, prism	colourless, prism	colourless, prism	colourless, prism
crystal size [mm ³]	0.06 × 0.06 × 0.03	0.21 × 0.21 × 0.03	0.21 × 0.18 × 0.15	0.12 × 0.09 × 0.06
crystal system	triclinic	monoclinic	monoclinic	monoclinic
<i>a</i> [Å]	8.6734(17)	12.851(3)	11.652(2)	13.622(3)
<i>b</i> [Å]	13.165(3)	10.384(3)	9.6047(18)	9.3562(18)
<i>c</i> [Å]	17.525(4)	29.473(8)	18.293(3)	17.224(4)
<i>α</i> [°]	102.307(6)	–	–	–
<i>β</i> [°]	96.444(6)	91.689(8)	92.268(5)	112.028(4)
<i>γ</i> [°]	93.395(4)	–	–	–
<i>V</i> [Å ³]	1935.7(7)	3931.5(18)	2045.6(6)	2034.9(8)
space group	<i>P</i> $\bar{1}$	<i>C2/c</i>	<i>P2₁/c</i>	<i>P2₁/n</i>
<i>Z</i>	4	8	4	4
ρ_{calcd} [g cm ^{−3}]	1.278	1.312	1.313	1.473
<i>F</i> (000)	784	1632	848	920
μ (MoK α) [cm ^{−1}]	0.254	2.57	3.446	20.33
no. of reflns measured	12 531	10 443	12 018	11 654
<i>R</i> _{int}	0.0595	0.044	0.06	0.075
min./max. transmissions	0.5879/1.000	0.946/0.992	0.928/0.950	0.779/0.885
independent reflns	6626	3418	3571	3570
observed reflns (no. variables)	3809 (470)	3044 (246)	3334 (246)	3162 (246)
refln/parameter ratio	14.1	13.89	14.52	14.51
<i>R</i> ₁ (<i>I</i> > 2.00 σ (<i>I</i>))	0.0614	0.0677	0.0658	0.069
<i>R</i> (all reflns)	0.1131	0.0844	0.0735	0.0808
<i>wR</i> ₂ (all reflns)	0.1245	0.2324	0.1767	0.1172
GOF	0.952	1.183	1.274	1.209
flack parameter	–	–	–	–
max. peak in final diff. map [e Å ^{−3}]	0.382	0.75	0.46	0.49
min. peak in final diff. map [e Å ^{−3}]	−0.332	−0.84	−0.42	−0.51

Table 8. Crystallographic data for compounds **2**, **2O**, **2S** and **2Se**.

	2	2O	2S	2Se
empirical formula	C ₂₈ H ₂₁ PS	C ₂₉ H ₂₃ OPSCl ₂	C ₂₈ H ₂₁ S ₂ P	C ₂₈ H ₂₁ PSSe
<i>M_r</i>	420.48	521.44	452.57	499.47
<i>T</i> [°C]	−180(1)	−148(1)	−148(1)	−148(1)
crystal colour, habit	colourless, platelet	colourless, prism	colourless, platelet	yellow, block
crystal size [mm ³]	0.10 × 0.10 × 0.10	0.09 × 0.09 × 0.09	0.18 × 0.12 × 0.06	0.15 × 0.12 × 0.12
crystal system	monoclinic	triclinic	monoclinic	monoclinic
<i>a</i> [Å]	11.1461(12)	9.2265(17)	9.3241(13)	9.432(4)
<i>b</i> [Å]	8.8914(10)	11.6406(16)	17.769(2)	17.849(6)
<i>c</i> [Å]	21.587(2)	13.239(3)	13.7930(19)	13.701(4)
<i>α</i> [°]	–	–	–	–
<i>β</i> [°]	90.837(4)	98.54(2)	97.328(3)	96.511(7)
<i>γ</i> [°]	–	112.23(2) ^o	–	–
<i>V</i> [Å ³]	2139.1(4)	1240.7(5)	2266.6(5)	2291.8(13)
space group	<i>P2₁/c</i>	<i>P</i> $\bar{1}$	<i>P2₁/n</i>	<i>P2₁/n</i>
<i>Z</i>	4	2	4	4
ρ_{calcd} [g cm ^{−3}]	1.306	1.396	1.326	1.447
<i>F</i> (000)	880	540	944	1016
μ (MoK α) [cm ^{−1}]	0.239	4.313	3.191	18.131
no. of reflns measured	13 424	12 814	12 358	12 375
<i>R</i> _{int}	0.0325	0.041	0.054	0.04
min./max. transmissions	0.8678/1.000	0.961/0.962	0.943/0.981	0.757/0.804
independent reflns	3774	4275	3948	4012
observed reflns (no. variables)	3348 (272)	3896 (308)	3521 (281)	3694 (281)
refln/parameter ratio	13.88	13.88	14.05	14.28
<i>R</i> ₁ (<i>I</i> > 2.00 σ (<i>I</i>))	0.0408	0.0508	0.0582	0.0427
<i>R</i> (all reflns)	0.0462	0.061	0.0694	0.0504
<i>wR</i> ₂ (all reflns)	0.1049	0.1469	0.123	0.1537
GOF	1.042	1.203	1.201	1.231
flack parameter	–	–	–	–
max. peak in final diff. map [e Å ^{−3}]	0.906	0.51	0.29	0.56
min. peak in final diff. map [e Å ^{−3}]	−0.314	−0.51	−0.36	−0.53

Table 9. Crystallographic data for compounds **3O**, **3S** and **3Se**.

	3O	3S	3Se
empirical formula	C ₂₈ H ₂₁ PSeO	C ₂₈ H ₂₁ PSeS	C ₂₈ H ₂₁ PSe ₂
<i>M</i> _r	483.41	499.47	546.37
<i>T</i> [°C]	−148(1)	−148(1)	−148(1)
crystal colour, habit	colourless, chunk	colourless, block	yellow, prism
crystal size [mm ³]	0.30 × 0.15 × 0.12	0.15 × 0.15 × 0.15	0.18 × 0.15 × 0.09
crystal system	monoclinic	monoclinic	monoclinic
<i>a</i> [Å]	10.1430(16)	9.3748(15)	9.4797(12)
<i>b</i> [Å]	10.6578(17)	17.820(3)	17.844(2)
<i>c</i> [Å]	10.6907(19)	13.847(2)	13.7175(16)
<i>α</i> [°]	—	—	—
<i>β</i> [°]	100.935(4)	97.820(5)	96.789(3)
<i>γ</i> [°]	—	—	—
<i>V</i> [Å ³]	1134.7(3)	2291.7(6)	2304.1(5)
space group	<i>P</i> 2 ₁	<i>P</i> 2 ₁ / <i>n</i>	<i>P</i> 2 ₁ / <i>n</i>
<i>Z</i>	2	4	4
<i>ρ</i> _{calcd} [g cm ^{−3}]	1.415	1.448	1.575
<i>F</i> (000)	492	1016	1088
<i>μ</i> (MoK _α) [cm ^{−1}]	17.43	18.132	32.93
no. of reflns measured	6648	13337	12528
<i>R</i> _{int}	0.029	0.034	0.051
min./max. transmissions	0.588/0.811	0.756/0.762	0.543/0.744
independent reflns	3674	4607	4046
observed reflns (no. variables)	3611 (281)	4279 (281)	3691 (281)
refln/parameter ratio	13.07	16.4	14.4
<i>R</i> ₁ (<i>I</i> > 2.00σ(<i>I</i>))	0.0374	0.0431	0.0553
<i>R</i> (all reflns)	0.0406	0.0486	0.065
<i>wR</i> ₂ (all reflns)	0.1131	0.087	0.1585
GOF	1.203	1.14	1.291
flack parameter	0.022(13)	—	—
max. peak in final diff. map [e Å ^{−3}]	0.69	0.41	0.71
min. peak in final diff. map [e Å ^{−3}]	−0.67	−0.45	−0.67

Acknowledgements

Elemental analyses were performed by Sylvia Williamson and mass spectrometry was performed by Caroline Horsburgh. Calculations were performed by using the EaStCHEM Research Computing Facility maintained by Dr. H. Früchtl. The work in this project was supported by the Engineering and Physical Sciences Research Council (EPSRC). Dr. Michael Bühl wishes to thank EaStCHEM for support.

- [1] a) H. E. Katz, *J. Am. Chem. Soc.* **1985**, *107*, 1420; b) R. W. Alder, P. S. Bowman, W. R. S. Steel, D. R. Winterman, *Chem. Commun.* **1968**, 723; c) T. Costa, H. Schimdbaur, *Chem. Ber.* **1982**, *115*, 1374; d) A. Karacar, M. Freytag, H. Thönnessen, J. Omelanczuk, P. G. Jones, R. Bartsch, R. Schmutzler, *Heteroat. Chem.* **2001**, *12*, 102; e) J. Meinwald, D. Dauplaise, F. Wudl, J. J. Hauser, *J. Am. Chem. Soc.* **1977**, *99*, 255; f) R. S. Glass, S. W. Andruski, J. L. Broecker, H. Firouzabadi, L. K. Steffen, G. S. Wilson, *J. Am. Chem. Soc.* **1989**, *111*, 4036; g) T. Fujii, T. Kimura and N. Furukawa, *Tetrahedron Lett.* **1995**, *36*, 1075; h) W. Nakanishi, S. Hayahi, S. Toyota, *Chem. Commun.* **1996**, 371; i) G. P. Schiemenz, *Z. Anorg. Allg. Chem.* **2002**, *628*, 2597; j) R. J. P. Corriu, J. C. Young in *The Chemistry of Organic Silicon Compounds* (Eds.: S. Patai, Z. Rappoport), Wiley, New York, **1989**, p. 1242.

- [2] a) C. A. Coulson, R. Daudel, J. M. Robertson, *Proc. R. Soc. London Ser. A* **1951**, *207*, 306; b) D. W. J. Cruickshank, *Acta Crystallogr.* **1957**, *10*, 504; c) C. P. Brock, J. D. Dunitz, *Acta Crystallogr. Sect. B* **1982**, *38*, 2218; d) J. Oddershede, S. Larsen, *J. Phys. Chem. A* **2004**, *108*, 1057.
- [3] V. Balasubramanian, *Chem. Rev.* **1966**, *66*, 567.
- [4] a) H. Schmidbaur, H.-J. Öller, D. L. Wilkinson, B. Huber, G. Müller, *Chem. Ber.* **1989**, *122*, 31; b) H. Fujihara, N. Furukawa, *J. Mol. Struct.* **1989**, *192–215*, 261; c) H. Fujihara, R. Akaishi, T. Erata, N. Furukawa, *J. Chem. Soc. Chem. Commun.* **1989**, 1789; d) J. Handal, J. G. White, R. W. Franck, Y. H. Yuh, N. L. Allinger, *J. Am. Chem. Soc.* **1977**, *99*, 3345; e) J. F. Blount, F. Cozzi, J. R. Damewood, D. L. Iroff, U. Sjöstrand, K. Mislow, *J. Am. Chem. Soc.* **1980**, *102*, 99; f) F. A. L. Anet, D. Donovan, U. Sjöstrand, F. Cozzi, K. Mislow, *J. Am. Chem. Soc.* **1980**, *102*, 1748; g) W. D. Hounshell, F. A. L. Anet, F. Cozzi, J. R. Damewood, Jr., C. A. Johnson, U. Sjöstrand, K. Mislow, *J. Am. Chem. Soc.* **1980**, *102*, 5941; h) R. Schroeck, K. Angermaier, A. Sladek, H. Schmidbaur, *Organometallics* **1994**, *13*, 3399.
- [5] F. R. Knight, A. L. Fuller, A. M. Z. Slawin, J. D. Woollins, *Chem. Eur. J.* **2010**, *16*, 7503–7516.
- [6] F. R. Knight, A. L. Fuller, A. M. Z. Slawin, J. D. Woollins, *Chem. Eur. J.* **2010**, *16*, 7605–7616.
- [7] P. Kilian, A. M. Z. Slawin, J. D. Woollins, *Dalton Trans.* **2003**, 3876.
- [8] E. Valls, J. Suades, *Organometallics* **1999**, *18*, 5475.
- [9] a) *Homogeneous Hydrogenation* (Ed.: B. R. James), Wiley Interscience, New York, **1973**; b) B. R. James, *Adv. Organomet. Chem.* **1979**, *17*, 319; c) *Organic Syntheses with Noble Metal Catalysts*, (Ed.: P. N. Rylander), Academic Press, New York, **1973**; d) J. L. Spencer, *Adv. Organomet. Chem.* **1979**, *17*, 407; e) A. J. Chalk, J. F. Harrod, *Adv. Organomet. Chem.* **1968**, *6*, 119; f) R. L. Pruet, *Adv. Organomet. Chem.* **1979**, *17*, 1; g) F. R. Hartley, *Chem. Rev.* **1969**, *69*, 799; h) P. M. Henry in *Palladium Catalyzed Oxidation of Hydrocarbons* (Ed.: D. Reidel), Springer, Dordrecht, **1979**; i) J. F. Roth, J. H. Craddock, A. Hershman, F. E. Paulik, *Chem. Technol.* **1971**, 600; j) D. Forster, *Adv. Organomet. Chem.* **1979**, *17*, 255.
- [10] a) R. D. Jackson, S. James, A. G. Orpen, P. G. Pringle, *J. Organomet. Chem.* **1993**, *458*, C3; b) S. L. James, A. G. Orpen, P. G. Pringle, *J. Organomet. Chem.* **1996**, *525*, 299; c) J. van Soolingen, R.-J. de Lang, R. den Besten, P. A. A. Klusener, N. Veldman, A. L. Spek, L. Brandsma, *Synth. Commun.* **1995**, *25*, 1741; d) E. Drent, J. A. M. van Broekhaven, M. J. Doyle, *J. Organomet. Chem.* **1991**, *417*, 235; e) G. P. C. M. Dekker, C. J. Elsevier, K. Vrieze, P. W. N. M. van Leeuwen, *Organometallics* **1992**, *11*, 1598; f) G. P. C. M. Dekker, C. J. Elsevier, K. Vrieze, P. W. N. M. van Leeuwen, C. F. Roobeek, *J. Organomet. Chem.* **1992**, *430*, 357; g) J. K. Hogg, S. L. James, A. G. Orpen, P. G. Pringle, *J. Organomet. Chem.* **1994**, *480*, c1; h) A. Karacar, H. Thönnessen, P. G. Jones, R. Bartsch, R. Schmutzler, *Chem. Ber. Rec.* **1997**, *130*, 1485; i) A. Karacar, H. Thönnessen, P. G. Jones, R. Bartsch, R. Schmutzler, *Heteroat. Chem.* **1997**, *8*, 539; j) H. B. Kagan in *Comprehensive Organometallic Chemistry, Vol. 8* (Ed.: G. Wilkinson), Pergamon Press, Oxford, **1982**, pp. 463–498; k) H. B. Kagan in *Asymmetric Synthesis, Vol. 5* (Ed.: J. D. Morrison), Academic Press, Orlando, **1985**, pp. 1–39; l) *Catalytic Asymmetric Synthesis* (Ed.: I. Ojima), Wiley-VCH, Weinheim, **1993**; m) *Asymmetric Catalysis in Organic Synthesis* (Ed.: R. Noyori), Wiley, New York, **1994**; n) R. Noyori, S. Hashiguchi in *Applied Homogenous Catalysis with Organometallic Compounds, Vol. 1* (Eds.: B. Cornils, W. A. Hermann), VCH, Weinheim, **1996**, p. 552; o) K. M. Pietrusiewicz, M. Zablocka, *Chem. Rev.* **1994**, *94*, 1375; p) A. Karacar, M. Freytag, H. Thönnessen, J. Omelanczuk, P. G. Jones, R. Bartsch, R. Schmutzler, *Heteroat. Chem.* **2001**, *12*, 102; q) W.-W. du Mont, R. Hensel, S. Kubiniok, L. Lange in *The Chemistry of Organic Selenium and Tellurium Compounds, Vol. 2* (Ed.: S. Patai), Wiley, New York, **1987**, Chapter 15; r) A. Karacar, M. Freytag, P. G. Jones, R. Bartsch, R. Schmutzler, *Z. Anorg. Chem.* **2001**, *627*, 1571.
- [11] a) G. P. Schiemenz, B. Schiemenz, S. Petersen, C. Wolff, *Chirality* **1998**, *10*, 180; b) D. Hellwinkel, W. Lindner, H.-J. Wilfinger, *Chem. Ber.* **1974**, *107*, 1428; c) D. Hellwinkel, W. Krapp, *Chem. Ber.* **1977**,

- 110, 693; d) R. O. Day, R. R. Holmes, *Inorg. Chem.* **1980**, *19*, 3609; e) A. Chandrasekaran, P. Sood, R. R. Holmes, *Inorg. Chem.* **1998**, *37*, 459; f) N. V. Timosheva, A. Chandrasekaran, R. O. Day, R. R. Holmes, *Inorg. Chem.* **1998**, *37*, 4945; g) C. Chuit, R. J. P. Corriu, P. Montforte, C. Réyé, J.-P. Declercq, A. Dubourg, *Angew. Chem.* **1993**, *105*, 1529; *Angew. Chem. Int. Ed. Engl.* **1993**, *32*, 1430; h) M. Chauhan, C. Chiut, R. J. P. Corriu, C. Reyé, J.-P. Declercq, A. Dubourg, *J. Organomet. Chem.* **1996**, *510*, 173; i) C. Chuit, R. J. P. Corriu, P. Montforte, C. Reyé, J.-P. Declercq, A. Dubourg, *J. Organomet. Chem.* **1996**, *511*, 171; j) C. Chuit, C. Reyé, *Eur. J. Inorg. Chem.* **1998**, 1847; k) G. P. Schiemenz, *Phosphorus Sulfur Silicon Relat. Elem.* **2000**, *163*, 185; l) G. Wittig, M. Rieber, *Liebigs Ann. Chem.* **1949**, *562*, 187; m) P. J. Wheatley, *J. Chem. Soc.* **1964**, 2206; n) G. P. Schiemenz, R. Bukowski, L. Eckholt, B. Varnskühler, *Z. Naturforsch. B* **2000**, *55*, 12; o) A. G. Eckstrand, *J. Prakt. Chem. N.F.* **1888**, *38*, 139; p) F. Dannerth, *J. Am. Chem. Soc.* **1907**, *29*, 1319; q) G. P. Schiemenz, S. Pörksen, C. Näther, *Z. Naturforsch. B* **2000**, *55*, 841; r) G. Dyker, M. Hagel, G. Henkel, M. Köckerling, C. Näther, S. Peterson, G. P. Schiemenz, *Z. Naturforsch. B* **2001**, *56*, 1109; s) G. P. Schiemenz, C. Näther, S. Pörksen, *Z. Naturforsch. B* **2003**, *58*, 663.
- [12] a) C. Chuit, R. J. P. Corriu, C. Reyé, J. C. Young, *Chem. Rev.* **1993**, *93*, 1371; b) C. Brelière, F. Carré, R. J. P. Corriu, M. Poirier, G. Royo, J. Zwecker, *Organometallics* **1989**, *8*, 1831; c) R. J. P. Corriu, J. C. Young in *The Chemistry of Organic Silicon Compounds* (Eds.: S. Patai, Z. Rappoport), Wiley, New York, **1989**, p. 1242; d) S. N. Tandura, M. G. Voronkov, N. V. Alekaev, *Top. Curr. Chem.* **1986**, *131*, 99; e) G. Sawiski, J. von Schnering, *Chem. Ber.* **1976**, *109*, 3728; f) C. Brelière, R. J. P. Corriu, G. Royo, J. Zwecker, *Organometallics* **1989**, *8*, 1834.
- [13] V. I. Minkin, *Pure Appl. Chem.* **1999**, *71*, 1919.
- [14] a) C. S. Slone, D. A. Weinberger, C. A. Mirkin, *Prog. Inorg. Chem.* **1999**, *48*, 233; b) P. Braunstein, F. Naud, *Angew. Chem.* **2001**, *113*, 702; *Angew. Chem. Int. Ed.* **2001**, *40*, 680; c) P. Espinet, K. Soulantica, *Coord. Chem. Rev.* **1999**, *193–195*, 499; d) J. C. Jeffrey, T. B. Rauchfuss, *Inorg. Chem.* **1979**, *18*, 2658; e) J. A. Davies, F. R. Hartley, *Chem. Rev.* **1981**, *81*, 79; f) T. B. Rauchfuss, F. T. Patino, D. M. Roundhill, *Inorg. Chem.* **1975**, *14*, 652.
- [15] a) S. M. Aucott, H. L. Milton, S. D. Robertson, A. M. Z. Slawin, G. D. Walker, J. D. Woollins, *Chem. Eur. J.* **2004**, *10*, 1666–1676; b) S. M. Aucott, H. L. Milton, S. D. Robertson, A. M. Z. Slawin, J. D. Woollins, *Heteroat. Chem.* **2004**, *15*, 530–542; c) S. M. Aucott, H. L. Milton, S. D. Robertson, A. M. Z. Slawin, J. D. Woollins, *Dalton Trans.* **2004**, 3347–3352; d) S. M. Aucott, P. Kilian, H. L. Milton, S. D. Robertson, A. M. Z. Slawin, J. D. Woollins, *Inorg. Chem.* **2005**, *44*, 2710–2718; e) S. M. Aucott, P. Kilian, S. D. Robertson, A. M. Z. Slawin, J. D. Woollins, *Chem. Eur. J.* **2006**, *12*, 895–902; f) S. M. Aucott, D. Duerden, Y. Li, A. M. Z. Slawin, J. D. Woollins, *Chem. Eur. J.* **2006**, *12*, 5495–5504.
- [16] a) P. Kilian, D. Philp, A. M. Z. Slawin, J. D. Woollins, *Eur. J. Inorg. Chem.* **2003**, 249–254; b) P. Kilian, A. M. Z. Slawin, J. D. Woollins, *Chem. Eur. J.* **2003**, *9*, 215–222; c) P. Kilian, A. M. Z. Slawin, J. D. Woollins, *Chem. Commun.* **2003**, 1174–1175; d) P. Kilian, H. L. Milton, A. M. Z. Slawin, J. D. Woollins, *Inorg. Chem.* **2004**, *43*, 2252–2260; e) P. Kilian, A. M. Z. Slawin, J. D. Woollins, *Inorg. Chim. Acta* **2005**, *358*, 1719; f) P. Kilian, A. M. Z. Slawin, J. D. Woollins, *Dalton Trans.* **2006**, 2175–2183.
- [17] F. R. Knight, A. L. Fuller, A. M. Z. Slawin, J. D. Woollins, *Polyhedron* **2010**, *29*, 1849–1858.
- [18] a) F. R. Knight, A. L. Fuller, A. M. Z. Slawin, J. D. Woollins, *Dalton Trans.* **2009**, 8476–8478; b) F. R. Knight, A. L. Fuller, A. M. Z. Slawin, J. D. Woollins, *Polyhedron* **2010**, *29*, 1956–1963.
- [19] W. Nakanishi, S. Hayashi, *Phosphorus Sulfur Silicon Relat. Elem.* **2002**, *177*, 1833.
- [20] H. Riihimäki, P. Suomalainen, H. K. Reinius, J. Suutari, S. Jääskeläinen, A. O. I. Krause, T. A. Pakkanen, J. T. Pursiainen, *J. Mol. Catal. A* **2003**, *200*, 69.
- [21] A. Bondi, *J. Phys. Chem.* **1964**, *68*, 441.
- [22] S. A. Reiter, S. D. Nogai, K. Karaghiosoff, H. Schmidbaur, *J. Am. Chem. Soc.* **2004**, *126*, 15833.
- [23] F. H. Allen, O. Kennard, D. G. Watson, L. Brammer, A. G. Orpen, R. Taylor, *J. Chem. Soc. Perkin Trans. 2* **1987**, S1.
- [24] P. Nagy, D. Szabó, I. Kapovits, Á. Kucsman, G. Argay, A. Kálmán, *J. Mol. Struct.* **2002**, *606*, 61.
- [25] a) W. Nakanishi, S. Hayashi, *J. Org. Chem.* **2002**, *67*, 38; b) S. Hayashi, K. Yamane, W. Nakanishi, *J. Org. Chem.* **2007**, *72*, 7587; c) W. Nakanishi, S. Hayashi, S. Toyota, *J. Am. Chem. Soc.* **1998**, *120*, 8790; d) W. Nakanishi, S. Hayashi, T. Uehara, *J. Phys. Chem. A* **1999**, *103*, 9906; e) W. Nakanishi, S. Hayashi, T. Uehara, *Eur. J. Org. Chem.* **2001**, 3933.
- [26] a) H. W. Roesky, M. Andruh, *Coord. Chem. Rev.* **2003**, *236*, 91; b) T. Koizumi, K. Tsutsui, K. Tanaka, *Eur. J. Org. Chem.* **2003**, 4528; c) C. Janiak, *J. Chem. Soc. Dalton Trans.* **2000**, 3885.
- [27] a) I. Vargas-Baca, T. Chivers, *Phosphorus Sulfur Silicon Relat. Elem.* **2000**, *164*, 207–227; b) N. Lozac'h, *Adv. Heterocycl. Chem.* **1971**, *13*, 161; c) R. E. Rosenfield, Jr., R. Parthasarathy, J. D. Dunitz, *J. Am. Chem. Soc.* **1977**, *99*, 4860; d) A. Kálmán, L. Párkányi, *Acta Crystallogr. Sect. B* **1980**, *36*, 2372; e) Á. Kucsman, I. Kapovits in *Organic Sulfur Chemistry: Theoretical and Experimental Advances* (Eds.: I. G. Csizmadia, A. Mangini, F. Bernardi), Elsevier, Amsterdam, **1985**, p. 191; f) J. G. Ángyán, R. A. Poirier, Á. Kucsman, I. G. Csizmadia, *J. Am. Chem. Soc.* **1987**, *109*, 2237; g) R. S. Glass, L. Adamowicz, J. L. Broeker, *J. Am. Chem. Soc.* **1991**, *113*, 1065; h) F. T. Burling, B. M. Goldstein, *Acta Crystallogr. Sect. B* **1993**, *49*, 738; i) Y. Nagao, T. Hirata, S. Goto, S. Sano, A. Kakehi, K. Iizuka, M. Shiro, *J. Am. Chem. Soc.* **1998**, *120*, 3104; j) K. Ohkata, M. Ohsugi, K. Yamamoto, M. Ohsawa, K. Akiba, *J. Am. Chem. Soc.* **1996**, *118*, 6355.
- [28] a) M. Nishio, *CrystEngComm* **2004**, *6*, 130; b) C. Fischer, T. Gruber, W. Seichter, D. Schindler, E. Weber, *Acta Crystallogr. Sect. E* **2008**, *64*, o673; c) M. Hirota, K. Sakaibara, H. Suezawa, T. Yuzuri, E. Ankaï, M. Nishio, *J. Phys. Org. Chem.* **2000**, *13*, 620; d) H. Tsubaki, S. Tohyama, K. Koike, H. Saitoh, O. Ishitani, *Dalton Trans.* **2005**, 385.
- [29] K. B. Wiberg, *Tetrahedron* **1968**, *24*, 1083.
- [30] 1,6-Dibromo-2-phenyl-1,2-diselenaacenaphthylene (two molecules in the unit cell with Se–Se distances of 2.516 and 2.542 Å): E. Horn, T. Nakahodo, N. Fukurawa, *Z. Kristallogr. New Cryst. Struct.* **2000**, *215*, 23.
- [31] S. D. Robertson, Ph.D. Thesis, University of St Andrews (UK), **2005**.
- [32] A. Karaçar, M. Freytag, H. Thönnessen, J. Omelanczuk, P. G. Jones, R. Bartsch, R. Schmutzler, *Z. Anorg. Allg. Chem.* **2000**, *626*, 2361.
- [33] D. Seyferth, S. C. Vick, *J. Organomet. Chem.* **1977**, *141*, 173.
- [34] H. O. House, D. G. Koepsell, W. J. Campbell, *J. Org. Chem.* **1972**, *37*, 1003.
- [35] CrystalClear v.1.6, Rigaku Corporation, **1999**; CrystalClear Software User's Guide, Molecular Structure Corporation, **2000**; J. W. P. Pflugrath, *Acta Crystallogr. Sect. D* **1999**, *55*, 1718.
- [36] A. Altomare, M. Burla, M. Camalli, G. Cascarano, C. Giacovazzo, A. Guagliardi, A. Moliterni, G. Polidori, R. Spagna, *J. Appl. Crystallogr.* **1999**, *32*, 115.
- [37] P. T. Beurskens, G. Admiraal, G. Beurskens, W. P. Bosman, R. de Gelder, R. Israel, J. M. M. Smits, The DIRDIF-99 program system, Technical Report of the Crystallography Laboratory, University of Nijmegen, Nijmegen, **1999**.
- [38] CrystalStructure v. 3.8.1, Crystal Structure Analysis Package, Rigaku and Rigaku/MS, Rigaku Americas, **2000–2006**.
- [39] G. M. Sheldrick, *Acta Crystallogr. Sect. A* **2008**, *64*, 112.
- [40] a) A. D. Becke, *J. Chem. Phys.* **1993**, *98*, 5648; b) C. Lee, W. Yang, R. G. Parr, *Phys. Rev. B* **1988**, *37*, 785.
- [41] R. C. Binning, L. A. Curtiss, *J. Comput. Chem.* **1990**, *11*, 1206.
- [42] A. E. Reed, L. A. Curtiss, F. Weinhold, *Chem. Rev.* **1988**, *88*, 899.
- [43] Gaussian 03, Revision E 01, M. J. Frisch, G. W. Trucks, H. B. Schlegel, G. E. Scuseria, M. A. Robb, J. R. Cheeseman, J. A. Montgomery, Jr., T. Vreven, K. N. Kudin, J. C. Burant, J. M. Millam, S. S. Iyengar, J. Tomasi, V. Barone, B. Mennucci, M. Cossi, G. Scalmani, N. Rega, G. A. Petersson, H. Nakatsuji, M. Hada, M. Ehara, K.

Toyota, R. Fukuda, J. Hasegawa, M. Ishida, T. Nakajima, Y. Honda, O. Kitao, H. Nakai, M. Klene, X. Li, J. E. Knox, H. P. Hratchian, J. B. Cross, V. Bakken, C. Adamo, J. Jaramillo, R. Gomperts, R. E. Stratmann, O. Yazyev, A. J. Austin, R. Cammi, C. Pomelli, J. W. Ochterski, P. Y. Ayala, K. Morokuma, G. A. Voth, P. Salvador, J. J. Dannenberg, V. G. Zakrzewski, S. Dapprich, A. D. Daniels, M. C. Strain, O. Farkas, D. K. Malick, A. D. Rabuck, K. Raghavachari, J. B. Foresman, J. V. Ortiz, Q. Cui, A. G. Baboul, S. Clifford, J. Cio-

slowski, B. B. Stefanov, G. Liu, A. Liashenko, P. Piskorz, I. Komaromi, R. L. Martin, D. J. Fox, T. Keith, M. A. Al-Laham, C. Y. Peng, A. Nanayakkara, M. Challacombe, P. M. W. Gill, B. Johnson, W. Chen, M. W. Wong, C. Gonzalez, J. A. Pople, Gaussian, Inc., Wallingford CT, **2004**.

Received: February 20, 2010
Published online: May 21, 2010